Synthesis, Structure and Electrochemistry of $Ph_2PCH_2PPh_2$-Bridged, Heterometallic Complexes containing a $(\eta\text{-}C_5H_4Me)Mn(CO)_2$ Fragment *,†

Pierre Braunstein,[a] Michael Knorr,[a] Martin Strampfer,[a] Yves Dusausoy,[b] Daniel Bayeul,[b] André DeCian,[c] Jean Fischer[c] and Piero Zanello[d]

[a] *Laboratoire de Chimie de Coordination, Associé au CNRS (URA 0416), Université Louis Pasteur, 4 rue Blaise Pascal, F-67070 Strasbourg Cédex, France*

[b] *Laboratoire de Minéralogie, Cristallographie et Physique Infrarouge, URA 809 CNRS, Université de Nancy I, F-54506 Vandoeuvre-les-Nancy Cédex, France*

[c] *Laboratoire de Cristallochimie et de Chimie Structurale, Associé au CNRS (URA 424), Université Louis Pasteur, 4 rue Blaise Pascal, F-67070 Strasbourg Cédex, France*

[d] *Dipartimento di Chimica dell' Università, Pian dei Mantellini 44, 53100 Siena, Italy*

Heterometallic complexes and clusters were prepared by using the new metallophosphine $[Mn(\eta\text{-}C_5H_4Me)(CO)_2(dppm\text{-}P)]$ **1** obtained from $[Mn(\eta\text{-}C_5H_4Me)(CO)_3]$ and $Ph_2PCH_2PPh_2$ (dppm). The dark green complexes $[(OC)_2(\eta\text{-}C_5H_4Me)Mn(\mu\text{-dppm})PdCl_2]$ and $[\{(\eta\text{-}C_5H_4Me)Mn(\mu\text{-}CO)_2(\mu\text{-dppm})Rh(\mu\text{-}Cl)\}_2]$, which contain metal–metal bonds, have been obtained by the reactions of **1** with $[PdCl_2(NCPh)_2]$ and $[\{Rh(cod)(\mu\text{-}Cl)\}_2]$ (cod = cycloocta-1,5-diene), respectively. Starting from $[Pt(cod)_2]$, the trimetallic complex $[Pt\{(\mu\text{-dppm})Mn(\eta\text{-}C_5H_4Me)(CO)_2\}_2]$ was formed and a reversible Mn–Pt bond formation has been observed by variable-temperature $^{31}P\text{-}\{^1H\}$ NMR spectroscopy. Reactions of **1** with $[PtCl_2(NCPh)_2]$, $[\{Re(CO)_3(thf)(\mu\text{-}Br)\}_2]$ (thf = tetrahydrofuran), $[\{RuCl(CO)_3(\mu\text{-}Cl)\}_2]$ and $[\{Ir(cod)(\mu\text{-}Cl)\}_2]$ led in high yields to complexes of the type Mn–dppm–M–dppm–Mn (M = Pt, Re, Ru or Ir) having no metal–metal interaction. With $[Mn(\eta\text{-}C_5H_4Me)(CO)_2(thf)]$, $[\{Pd(\eta^3\text{-}C_3H_4Me)(\mu\text{-}Cl)\}_2]$ or [AuBr(tht)] (tht = tetrahydrothiophene) bimetallic complexes of the type Mn–dppm–M′ (M′ = Mn, Pd or Au) were obtained again with no metal–metal interaction. Another route to this type of bimetallic complexes consists of the reaction of $[(OC)_2(\eta\text{-}C_5H_4Me)Mn(\mu\text{-dppm})PdCl_2]$ with two-electron donor ligands such as isocyanides RNC (R = 2,6-xylyl or Bu^t), which yielded $[(OC)_2(\eta\text{-}C_5H_4Me)Mn(\mu\text{-dppm})Pd(CNR)Cl_2]$. Reaction of the isocyanide complexes with azetidine did not lead to the expected carbene complexes, instead the isocyanide ligand was substituted by azetidine, yielding $[(OC)_2(\eta\text{-}C_5H_4Me)Mn(\mu\text{-dppm})Pd(NHC_3H_6)Cl_2]$. The structures of the xylyl isocyanide and azetidine complexes have been determined by X-ray diffraction. Reaction of $[(OC)_2(\eta\text{-}C_5H_4Me)Mn(\mu\text{-dppm})AuBr]$ with the metalate $K[Fe\{Si(OMe)_3\}(CO)_3(PPh_3)]$ gave in high yield the heterotrimetallic chain complex $[(OC)_2(\eta\text{-}C_5H_4Me)Mn(\mu\text{-dppm})AuFe\{Si(OMe)_3\}(CO)_3(PPh_3)]$. Reaction of **1** with *trans*-$[Pt\{W(\eta\text{-}C_5H_4Me)(CO)_3\}_2(NCPh)_2]$ afforded the cluster $[Pt_2W_2(\eta\text{-}C_5H_4Me)_2(\mu_3\text{-}CO)_2(\mu\text{-}CO)_4\{(\mu\text{-dppm})Mn(\eta\text{-}C_5H_4Me)(CO)_2\}_2]$. An electrochemical study of some of the complexes has provided evidence for possible electronic communication between the metal centres.

Considerable progress has been made over the last years in developing the systematic use of organometallic building blocks to prepare molecular mixed-metal clusters in high yields, which facilitates the study of their site-selective reactivity and of synergistic effects. Establishing relationships between reactivity patterns and structural features remains a prime objective in this chemistry.[1] Strategies based on the use of assembling ligands have been very successful for the stepwise construction of complex molecules. Thus, a convenient method for preparing heterometallic complexes consists of the reaction of a mononuclear precursor containing a pendant $Ph_2PCH_2PPh_2$ (dppm) ligand with a second metal centre. In addition to a stabilizing role of the dppm backbone, formation of a metal–metal interaction is often observed.[2] As part of our studies on silicon-containing heterometallic complexes, we recently described the use of the hydridosilyl complexes $[FeH\{Si(OR)_3\}(CO)_3(dppm\text{-}P)]$ (R = Me or Et) and the derived metalates $K[Fe\{Si(OR)_3\}(CO)_3(dppm\text{-}P)]$ for the construction of dppm-bridged, heterometallic arrays.[3] In this paper we report on a new series of heterometallic chain complexes and clusters prepared from the 'metallophosphine' $[Mn(\eta\text{-}C_5H_4Me)(CO)_2(dppm\text{-}P)]$ **1** in which the diphosphine acts as a monodentate ligand. Only a few phosphorus-bridged complexes containing the $Mn(C_5H_5)(CO)_2$ fragment have been described which contain[4] or not[5] metal–metal bonds.

The reversibility of the reduction of the 17-electron complexes $[Cr(\eta\text{-}C_5R_5)(CO)_2(PR_3)]$ to the corresponding 18-electron metalates $[Cr(\eta\text{-}C_5R_5)(CO)_2(PR_3)]^-$ has been electrochemically ascertained[6,7] and the crystal structures of the redox partners are available.[7b,8,9] As far as the corresponding manganese complexes are concerned, electrochemical investigations of the 18-electron species $[Mn(\eta^5\text{-}C_5R_5)(CO)_2(PR_3)]$ have presented the possibility of obtaining the 17-electron congeners $[Mn(\eta\text{-}C_5R_5)(CO)_2(PR_3)]^+$.[10] We report here an electrochemical study of the 18-electron manganese(I) complex **1** and of some of its bi-, tri-, tetra- and hexa-nuclear complexes.

* Part of the Doctoral Thesis of M. S., University of Strasbourg, 1993.
† *Supplementary data available:* see Instructions for Authors, *J. Chem. Soc., Dalton Trans.*, 1994, Issue 1, pp. xxiii–xxviii.

The redox behaviour of the somewhat related complex [Mn(CN)(CO)$_2$(PR$_3$)(dppm-*P*,*P*′)] and of its polynuclear derivatives has been investigated.[11]

Results and Discussion

Preparation of [Mn(η-C$_5$H$_4$Me)(CO)$_2$(dppm-*P*)] **1**.—The reaction of [Mn(η-C$_5$H$_4$Me)(CO)$_2$(thf)] (thf = tetrahydrofuran) with 1 equivalent of dppm afforded a mixture of complex **1** and [{Mn(η^5-C$_5$H$_4$Me)(CO)$_2$}$_2$(μ-dppm)] **2** in a 60:40 ratio (by ^{31}P-{^{1}H} NMR integration) [equation (1)]. This mixture

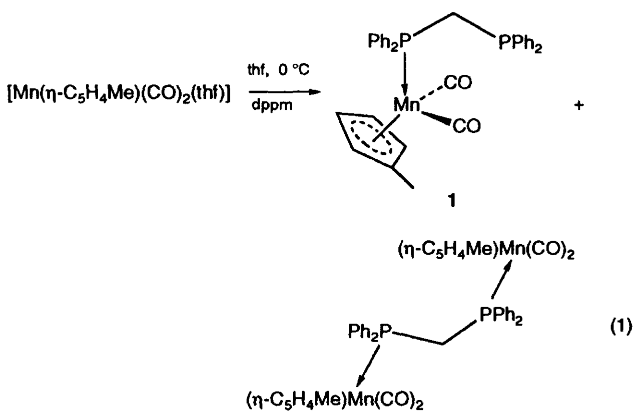

1

(1)

2

can be separated by column chromatography. The presence of a monodentate dppm ligand in **1** is confirmed by the AX pattern observed in the ^{31}P-{^{1}H} NMR spectrum in which the doublet for the pendant phosphorus atom is found in the typical range for an unco-ordinated phosphorus nucleus at δ −26.3 [^2J(P–P) = 77 Hz] and the quadrupolar broadened resonance for the manganese-bound phosphorus atom at δ 85.5. In contrast, a singlet resonance at δ 88.5 is observed for **2**, a value similar to the chemical shift of δ 81.3 for [Mn$_2$(μ-η^5:η^5-C$_5$H$_4$=C$_5$H$_4$)(CO)$_4$(μ-dppm)].[12a] The two IR ν(CO) absorptions for **1** and **2** cm^{-1} are of similar intensities, indicating a C–Mn–C angle close to 90°.[13] Yellow, air-stable **1** and **2** are scarcely soluble in hexane but very soluble in diethyl ether and aromatic solvents. Slow addition of [Mn(η-C$_5$H$_4$Me)(CO)$_2$H-(SiPh$_3$)][12b] to a stirred toluene solution at 60 °C containing 1 equivalent of dppm also afforded a mixture of **1** and **2**. The metallophosphine **1** was used to prepare new heterometallic complexes which will be presented below according to the bonding mode of **1** in these complexes. Thus, the occurrence of a manganese–metal interaction makes **1** behave as a formal four-electron donor and such complexes will be presented first. When **1** is only bound to the heterometal through the phosphorus lone pair it behaves as a two-electron donor and the crystal structures of complexes **12a** and **13** will be detailed. Examples of the conversion of complexes of the former class into the latter will also be presented. Finally, electrochemical data on some of these complexes will be discussed.

Reactions of Complex **1** *with Complexes of* Pd^{II}, Pt^0 *and* Rh^I *affording Metal–Metal Bonded Complexes*.—The reaction of complex **1** with a slight excess of [PdCl$_2$(NCPh)$_2$] in toluene afforded dark green, air-stable [(OC)$_2$(η-C$_5$H$_4$Me)-Mn(μ-dppm)PdCl$_2$] **3** in good yields [equation (2)]. This

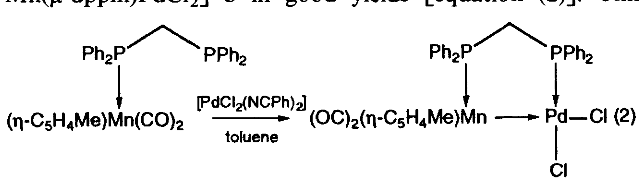

(2)

1 3

intense colour appears typical of the presence of a metal–metal bond, resulting from a donor–acceptor interaction between the filled d orbitals (t_{2g} set) of the manganese atom and the appropriate vacant orbital on Pd, allowing this metal to reach a 16-electron configuration. A related situation is observed in the green complex [(dppm-*P*,*P*)(OC)$_3$Mo(μ-dppm)PdCl$_2$].[14] The presence of a bridging dppm ligand in **3** is confirmed by the AX pattern observed in the ^{31}P-{^{1}H} NMR spectrum in which the doublet for the palladium-bound phosphorus atom is found at δ 40.5 [^{2+3}J(P–P) = 61 Hz] and the quadrupolar broadened doublet resonance for the manganese-bound phosphorus atom at δ 89.8. The presence of a Mn–Pd bond is also evidenced by the relatively large ^{2+3}J(P–P) coupling constant when compared to the values found in complexes without Mn–M interaction (see below). The relatively low ν(Pd–Cl) absorptions observed at 299 and 282 cm^{-1} are characteristic for a *cis* arrangement of the chlorides, the ν(Pd–Cl) stretches of *e.g.* *trans*-[PdCl$_2$(PPh$_3$)$_2$] being found at 358 cm^{-1} and of *cis*-[PdCl$_2$(dppe)] (dppe = Ph$_2$PCH$_2$CH$_2$PPh$_2$) at 310 and 286 cm^{-1}.[15] The ν(CO) values for **3** are sufficiently similar to those of **1** to rule out any significant bridging interaction between the CO groups and the palladium centre. The integral intensity ratio of the symmetric and antisymmetric (1896, 1850 cm^{-1}) carbonyl stretches is approximately 0.35:1, corresponding to a C–Mn–C angle of 120°.[13] Two different geometries have been previously discussed for (C$_5$H$_5$)ML$_4$ fragments and compared by extended-Hückel calculations: the lowest-energy geometry was found[16] to be a four-legged piano-stool **A** with C_{4v} symmetry, whereas a capped trigonal bipyramid **B** with C_{3v}

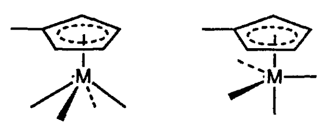

A **B**

symmetry lies at higher energy. However, the energy difference between types **A** and **B** is expected to be small and a diagonal (*trans*) arrangement of the carbonyls in a structure of type **A** cannot be ruled out by spectroscopic methods. Bimetallic Mn–M complexes have been found to display type **A** or **B** geometries and the influence of steric factors should be kept in mind.[16,17] It is interesting to compare the (η-C$_5$H$_4$Me)Mn(CO)$_2$L fragment with its isoelectronic analogues [M(η-C$_5$H$_5$)(CO)$_3$]$^-$ (M = Cr, Mo or W) which readily form metal–metal bonds and generally behave as two-electron donors or, more rarely, as four-electron donors, as in [Pd$_2$(or Pt$_2$)M$_2$(η-C$_5$H$_5$)$_2$(CO)$_6$(PR$_3$)$_2$] (M = Cr, Mo or W).[18–20]

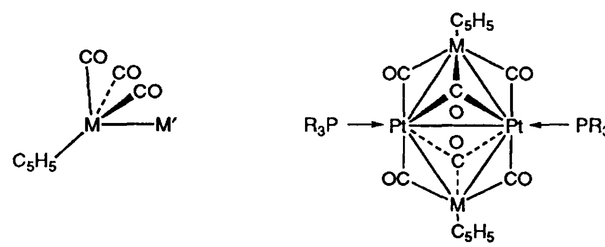

Two electron donor metalate

M = Cr, Mo, or W
Four electron donor metalate

Addition of 1 equivalent of complex **1** to **3** did not lead to the displacement of the Mn→Pd interaction with formation of a trinuclear complex, but rather decomposition to mononuclear species. However, the dative Mn→Pd bond in **3** was readily split by other two-electron donor ligands (see below).

The reaction of 2 equivalents of complex **1** with [Pt(cod)$_2$] (cod = cycloocta-1,5-diene) resulted in the orange complex

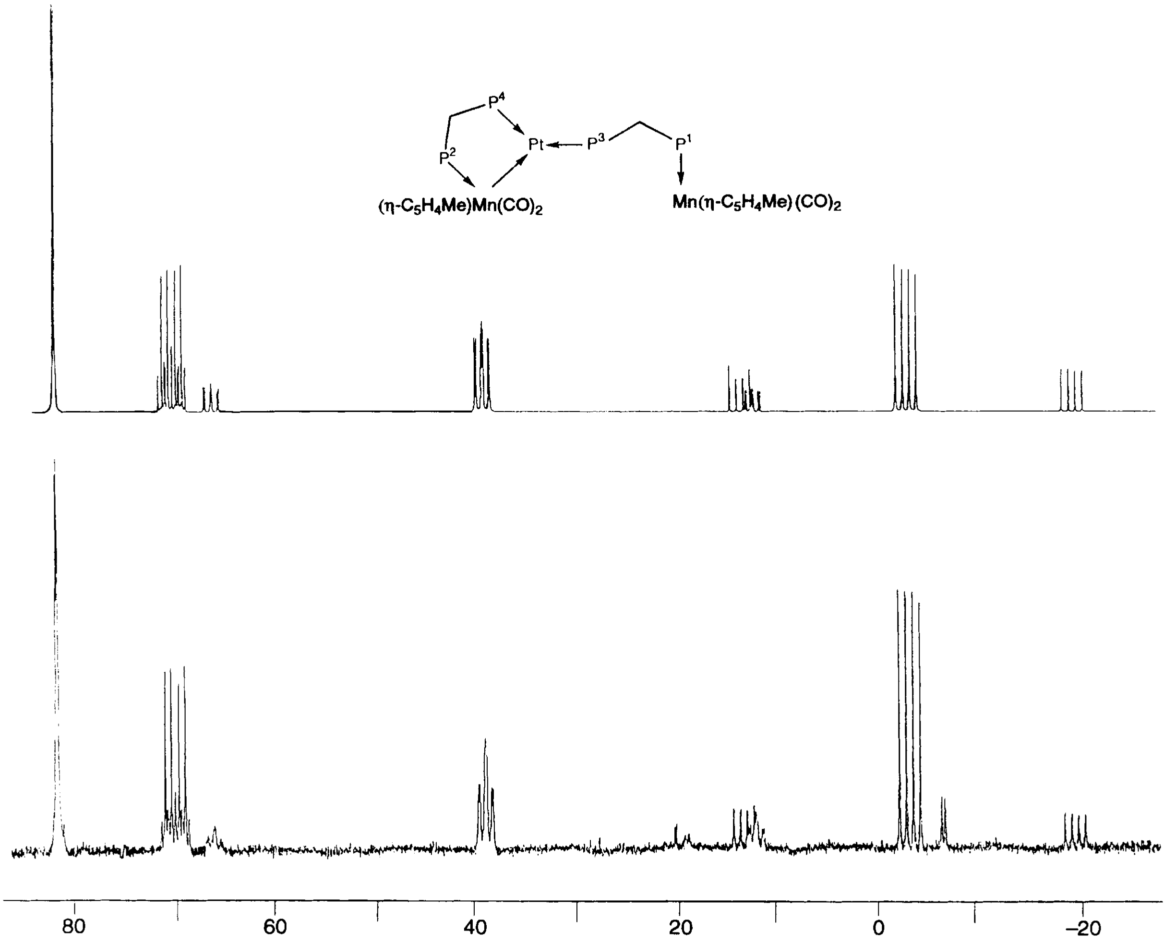

Fig. 1 ^{31}P-{^{1}H} NMR spectrum of the complex [Pt{(μ-dppm)Mn(η-C_5H_4Me)(CO)$_2$}$_2$] **4** in CH_2Cl_2–C_6D_6 at 253 K (bottom). Spectral simulation was performed with the PANIC program (Bruker) (top)

[Pt{(μ-dppm)Mn(η-C_5H_4Me)(CO)$_2$}$_2$] **4**. This compound shows a dynamic behaviour at ambient temperature [equation (3)], giving rise in the ^{31}P-{^{1}H} NMR spectrum to two very broad signals in the characteristic regions of phosphorus atoms bound to Mn (δ *ca.* 82) and Pt (δ *ca.* 50 to −10). However at 253 K a well resolved spectrum could be obtained (Fig. 1) which was interpreted to a first approximation in terms of a first-order spectrum. However, the coupling constants were determined by spectral simulation. There are two types of diphosphine ligands bound to platinum and manganese, one showing a strong, the other a weak (P–P) coupling. The strong (P^2–P^4) coupling of 112 Hz corresponds to a ^{2+3}J coupling and therefore to a dppm ligand supporting a manganese–platinum bond, whereas the weaker (P^1–P^3) coupling of 13.1 Hz is due to a ^2J coupling of a Mn(μ-dppm)Pt unit without any direct Pt–Mn interaction. The presence of a metal–metal bond is further supported by the observation of a ^{2+3}J(P^2–Pt) coupling of 58 Hz involving one of the manganese-bound phosphorus atoms, whereas the other P^1(Mn) does not display such a coupling. Furthermore a ^{3+4}J(P^2–P^3) coupling of 50 Hz is observed for only one of the Mn-bound phosphorus atoms. These results suggest for **4** a low-temperature structure as drawn in equation (3), with a dynamic formation and breaking of Pt–Mn bonds occurring at higher temperatures. No exchange was observed between **1** and **4**, since an excess of **1** in a CH_2Cl_2 solution of **4** maintained the sharp ^{31}P-{^{1}H} NMR resonances for **1**.

It is surprising that the CO stretches are so little affected by this behaviour, only two absorptions being observed at 1922 and 1856 cm^{-1}. The FIR spectrum of complex **4** contains a strong band at 121 cm^{-1} which is absent in the spectrum of **1** and

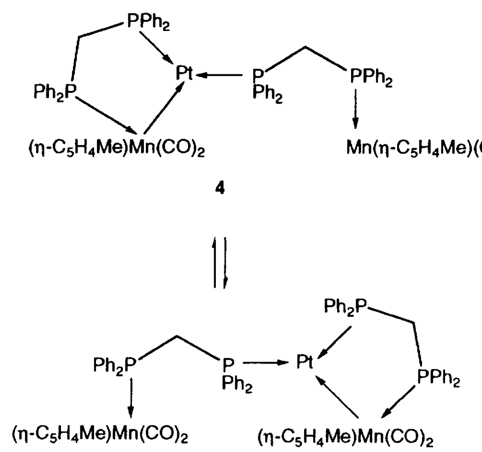

(3)

might be therefore tentatively assigned to the metal–metal vibration. The 16e platinum centre should have the Y shape geometry usually encountered in platinum(0) species.[21] Relatively few examples of intramolecular, reversible bond breaking/formation processes are known for heterometallic clusters and the relevance of this phenomenon to potential catalytic processes involving heterometallic clusters has been discussed.[22] Upon stirring **1** in a CH_2Cl_2 solution with an excess of [Pt(C_2H_4)(PPh_3)$_2$] for several days, **4** was formed besides other products which were not characterized. Interestingly, both starting materials were still present in solution indicating the limited reactivity of **1**. When **4** was treated with CO or a stoichiometric amount of RNC (R = 2,6-xylyl) or $AsPh_3$, $^{31}P-\{^1H\}$ NMR monitoring indicated decomposition yielding **1** as the main phosphorus-containing product.

Reaction of 2 equivalents of complex **1** with $[\{Rh(cod)(\mu-Cl)\}_2]$ yielded the dark green complex $[\{(\eta-C_5H_4Me)Mn(\mu-CO)_2(\mu-dppm)Rh(\mu-Cl)\}_2]$ **5** in good yields. The carbonyl stretches at 1783 and 1750 cm^{-1} suggest a bridging mode for the carbonyl groups. In the $^{31}P-\{^1H\}$ NMR spectrum the ddd resonance at δ 52.4 is assigned to the Rh-bound phosphorus atom [$^1J(P-^{103}Rh)$ 164 Hz is in the usual range[23a]] and shows a $^{2+3}J(P-P)$ coupling of 77 Hz and a further splitting of *ca.* 2 Hz. No coupling to ^{103}Rh larger than 10 Hz is detected for the Mn-bound phosphorus (δ 94.7). The FAB^+ mass spectrum shows a peak at *m/z* 1368 which corresponds to $[M - 2CO]^+$ and is the only one displaying the typical pattern due to the presence of chlorine. Some other peaks due to fragments containing no chlorine groups are also observed (see Experimental section), which may be due to rearrangement reactions in the matrix. After only one scan, run less than 1 min after sample preparation, the peaks corresponding to **5** and its rearrangement products in a $p-O_2NC_6H_4CH_2OH$–thf matrix disappeared whereas a peak at *m/z* 1060 gradually increased and remained the highest-mass peak after 10 scans (*ca.* 3 min). It may be assigned by its isotopic pattern to a species $[(OC)_2(\eta-C_5H_4Me)Mn(\mu-dppm)Rh(dppm)]^+$ which contains no chlorine atom. The ν(Rh–Cl) stretches at 264 and 255 cm^{-1} compare with those of $[\{Rh(cod)(\mu-Cl)\}_2]$ at 278 and 260 cm^{-1} [24] and are therefore indicative of the presence of bridging chlorine atoms. We suggest for **5** the dimeric structure shown below with two Mn–Rh units connected to each other by chloride bridges, similar to the structure proposed for $[\{(\eta-C_5H_5)Fe(\mu-CO)_2(\mu-dppm)Rh(\mu-Cl)\}_2][BF_4]_2$.[23b] The coupling constant of 2 Hz would then correspond to a $^3J(P-Rh)$ coupling through the chloride bridges; however, it was not detected in the Fe–Rh complex. When assuming a dative Mn→Rh interaction in **5** the manganese and rhodium atoms reach a 18-electron configuration. Only few six-co-ordinated rhodium(I) complexes have been characterized due to their generally limited stability.[25] Reaction of 4 equivalents of **1** with $[\{Rh(cod)(\mu-Cl)\}_2]$ led after prolonged stirring in toluene to an equilibrium consisting of a poorly soluble product formulated as $[\{[(OC)_2(\eta-C_5H_4Me)Mn(\mu-dppm)]_2Rh(\mu-Cl)\}_2]$ **6** and some unreacted **1** and **5**. The $^{31}P-\{^1H\}$ NMR spectrum of **6** in CH_2Cl_2 shows a quadrupole-broadened singlet resonance at δ 87.1 and a doublet of 'triplets' at δ 21.2. The large coupling of 126 Hz in the latter corresponds to a $^1J(P-Rh)$ and the triplets to a 'deceptively simple' form[26] of the expected AA′XX′ pattern [$N = |^2J(P_AP_X) + ^4J(P_AP_{X'})| = 14$ Hz]. We therefore propose a dimeric structure for **6** with bridging μ-Cl groups [unfortunately no ν(Rh–Cl) absorptions were detected in the FIR spectrum] and a planar co-ordination for the Rh with the phosphorus atoms being in a *cis* arrangement.[27] Complex **6** was also obtained upon splitting of the metal–metal bond of **5** by addition of 2 equivalents of **1**. The reversibility of equation (4) was independently shown by dissolving pure **6** in CH_2Cl_2 and following by $^{31}P-\{^1H\}$ NMR spectroscopy its transformation into **5** and **1**. A complex similar to **6** was isolated with Ir instead of Rh (see below).

Reactions of Complex **1** *with Complexes of* Pt, Re, Ru, Ir, Au *and* Pd, *affording Products without Metal–Metal Interactions.*— As shown above, complex **1** can be used for the construction of metal–metal bonded complexes. Another class of compounds could be synthesised in which there is no direct interaction of the filled d orbitals of the manganese atom with the adjacent metal. The characteristics of these complexes are: (*i*) pale colours similar to those of the starting materials, (*ii*) minor changes of the ν(CO) stretches compared to **1** and (*iii*) small $^2J(P-P)$ coupling constants in the $^{31}P-\{^1H\}$ NMR spectra.

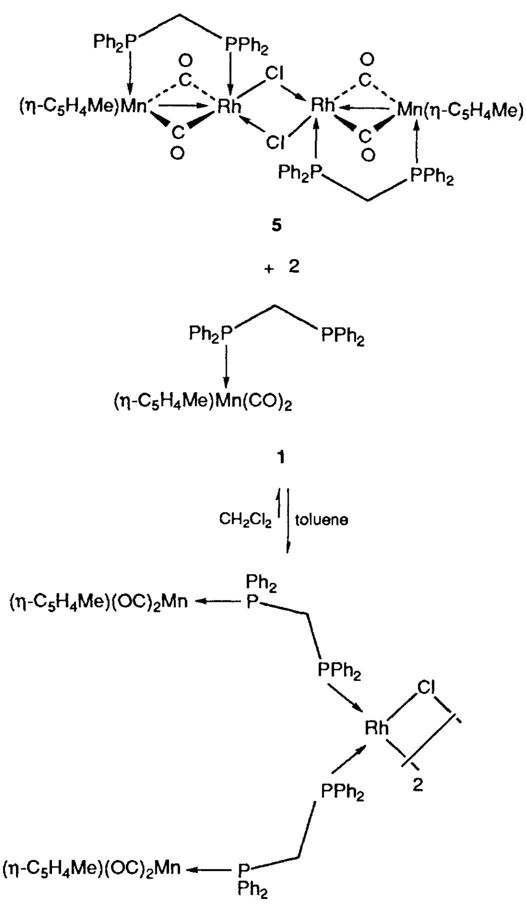

6 (4)

The reaction of 2 equivalents of complex **1** with $[PtCl_2(NCPh)_2]$ in toluene gave the crystalline, yellow product *trans*-$[PtCl_2\{(\mu-dppm)Mn(\eta-C_5H_4Me)(CO)_2\}_2]$ **7** in good yields. There was no evidence for the formation of a compound similar to **3** even when **1** was added slowly or when $[PtCl_2(NCPh)_2]$ was used in excess. The IR spectrum in the carbonyl region of **7** showed no significant change compared to **1**. The $^{31}P-\{^1H\}$ NMR spectrum displays a quadrupole-broadened singlet resonance at δ 88.4 for the manganese-bound phosphorus atoms (no couplings being resolved), whereas the platinum-bound phosphorus atoms give rise to a 'triplet' resonance at δ 6.6. Such a pattern has previously been interpreted as a 'deceptively simple' example of an AA′XX′ spin system in similar complexes (the coupling *N* corresponds to the separation between the outer resonances, *N* = 23 Hz).[26] These phosphorus atoms are coupled to ^{195}Pt with a $^1J(P-Pt)$ of 2579 Hz, a normal value for *trans*-$[PtX_2(PR_3)_2]$ complexes.[28] A comparable spectrum was recently observed for a Mo–POP–Pd–POP–Mo (POP = Ph_2POPPh_2)[29a] and a Au–dppm–Pt–dppm–Au array.[29b] By comparison with the FIR spectrum of **2**, the strong absorption detected at 357 cm^{-1} could be assigned to the ν(Pt–Cl) of a *trans*-$PtCl_2$ unit. In the ^1H NMR spectrum of **7** the chemical shift of the PCH_2P resonance is solvent dependent, being at δ 4.38 in C_6D_6 and below δ 4.0 in CD_2Cl_2.

When $[\{Re(CO)_3(thf)(\mu-Br)\}_2]$ was treated in a similar manner with 2 equivalents of complex **1**, $[ReBr(CO)_3\{(\mu-dppm)Mn(\eta-C_5H_4Me)(CO)_2\}_2]$ **8** was formed in high yields. In the FAB^+ mass spectrum the molecular peak is detected at *m/z* 1499, $[M + H]^+$. The IR spectrum contains strong absorptions at 1925 and 1860 cm^{-1} due to the $(\eta-C_5H_4Me)Mn(CO)_2$ moiety and at 2025, 1940 and 1907 cm^{-1} corresponding to the rhenium carbonyls, the last two bands partly overlapping with those of the manganese carbonyls. This is consistent with a *fac*

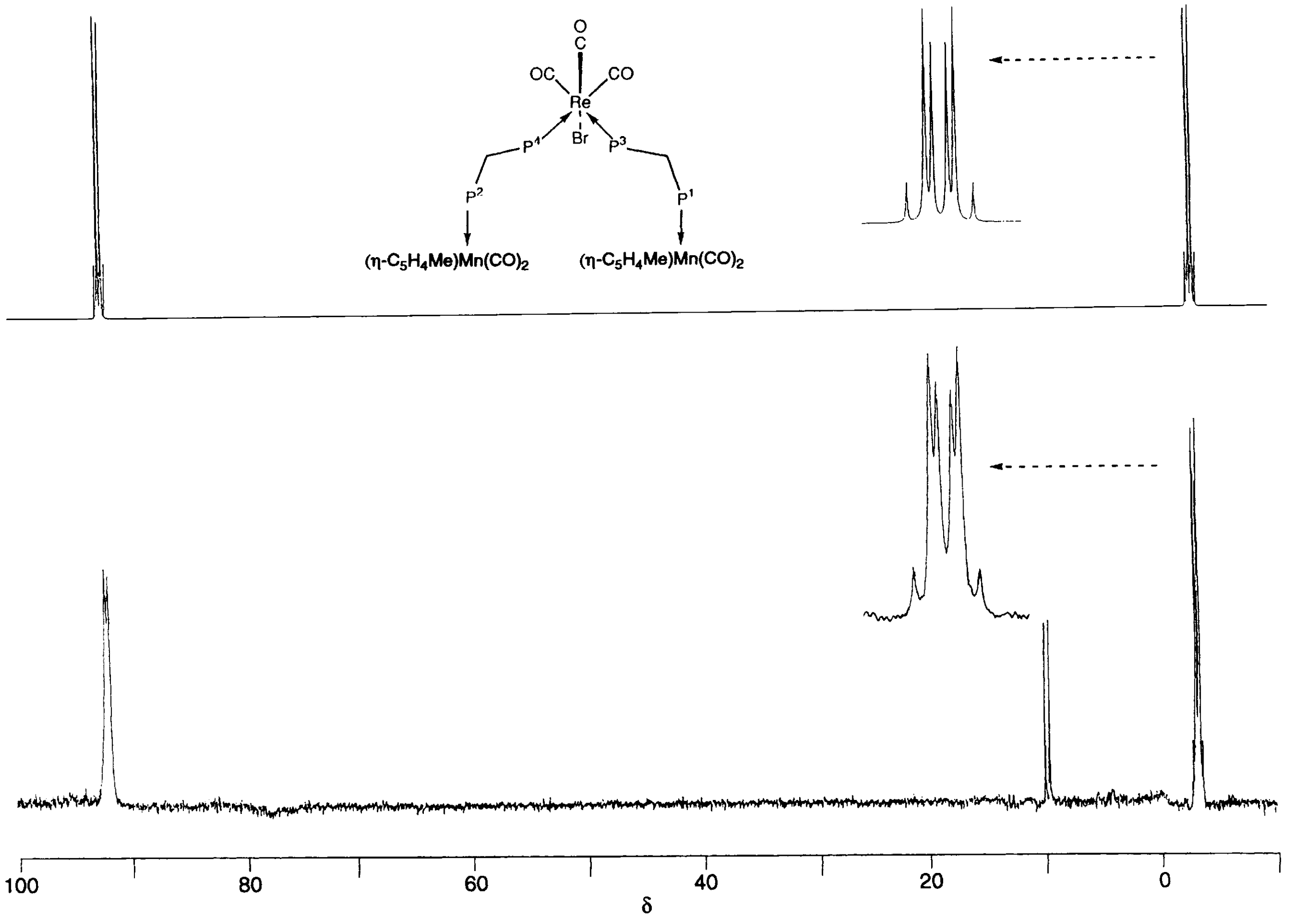

Fig. 2 The $^{31}P-\{^1H\}$ NMR spectrum of $[ReBr(CO)_3\{(\mu\text{-dppm})Mn(\eta\text{-}C_5H_4Me)(CO)_2\}_2]$ **8** in CH_2Cl_2–C_6D_6 at room temperature (bottom). Spectral simulation as in Fig. 1 (top)

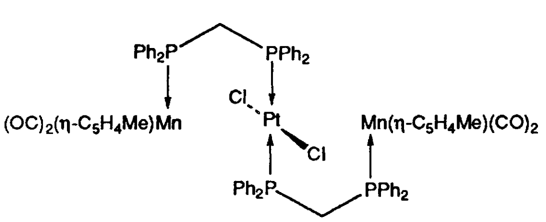

7

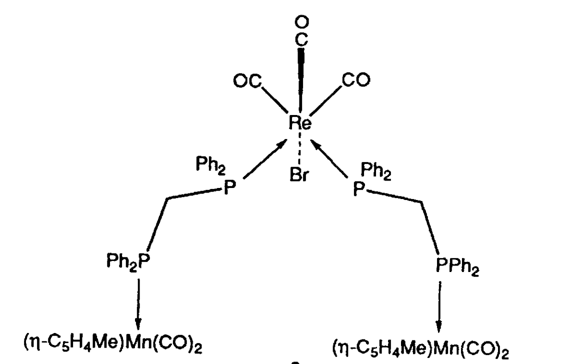

8

arrangement of the rhenium carbonyls,[30] as was also found in $[ReBr(CO)_3(dppm\text{-}P,P)]$ [$^{31}P-\{^1H\}$ NMR (C_6D_6–toluene): δ −36.7; lit.,[30c] −38.5. ν(CO) (KBr): 2025vs, 1943s and 1905s cm^{-1}; FIR (polyethylene) ν(Re–Br) 198 cm^{-1}]. In the FIR spectrum of **8** the ν(Re–Br) stretch is detected at 186 cm^{-1}. The $^{31}P-\{^1H\}$ NMR spectrum displays two typical multiplets at δ 91.0 and −3.9. Spectral simulation of this AA′XX′ spin system afforded the coupling constants $^4J(P^1\text{–}P^3)$ = −0.5 Hz, $^2J(P^1\text{–}P^4)$ = 31.0, $^2J(P^2\text{–}P^3)$ = 31.6, $^4J(P^2\text{–}P^4)$ = −1.1 and $^2J(P^3\text{–}P^4)$ = 26.2 Hz (Fig. 2). From these data we propose for **8** the structure illustrated.

Even slow addition of complex **1** to a cold dichloromethane solution of an excess of $[\{Re(CO)_3(thf)(\mu\text{-}Br)\}_2]$ gave mainly **8**; only a small quantity (*ca.* 15%) of another product was detected by $^{31}P-\{^1H\}$ NMR spectroscopy but could not be isolated. Its spectrum contains a doublet resonance for the P(Re) at δ 9.5 [*J*(P–P) = 30 Hz] and a P(Mn) resonance which would coincide with that of **8**, possibly indicating the presence of some $[\{(OC)_2(\eta\text{-}C_5H_4Me)Mn(\mu\text{-dppm})Re(CO)_3(\mu\text{-}Br)\}_2]$. This would be consistent with previous findings indicating that the thf ligand of $[\{Re(CO)_3(thf)(\mu\text{-}Br)\}_2]$ is substituted before cleavage of the halide bridge occurs.[30f]

Reaction of 2 equivalents of complex **1** with $[\{RuCl(CO)_3(\mu\text{-}Cl)\}_2]$ gave the new yellow complex $[RuCl_2(CO)_2\{(\mu\text{-dppm})Mn(\eta\text{-}C_5H_4Me)(CO)_2\}_2]$ **9**. Its IR spectrum displays in the ν(CO) region two sets of absorptions: the first at 2055 and 1991 cm^{-1} with equal intensities indicates an angle between the two ruthenium carbonyls close to 90° (*cis* arrangement). The second set of very strong absorptions at 1925 and 1858 cm^{-1} corresponds to the almost unperturbed $(\eta\text{-}C_5H_4Me)Mn(CO)_2$ fragments. The $^{31}P-\{^1H\}$ NMR spectrum displays a quadrupole-broadened resonance at δ 89.8 for the manganese-bound phosphorus atoms and a four-line pattern (apparent doublet of doublets) at δ 17.7 for the ruthenium-bound phosphorus atoms (*N* = 34 Hz). A $^{31}P-\{^1H\}$ NMR spectrum recorded at 160 MHz proved that the multiplets belong to only one AA′XX′ spin system and that the splittings between the lines correspond to coupling constants. This implies two chemically equivalent Ru-bound phosphorus atoms and a *trans* arrangement for the

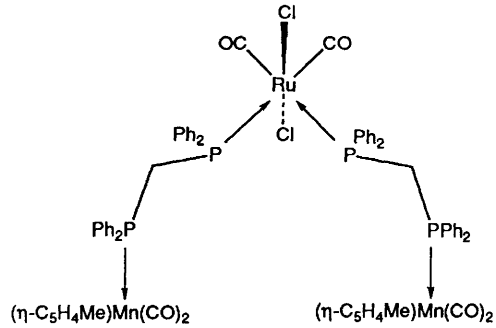

9

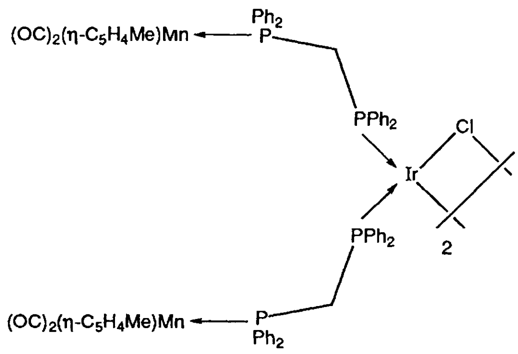

10

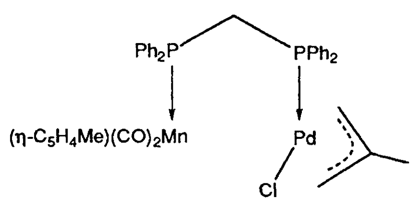

11

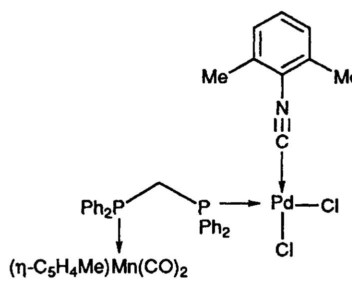

12a

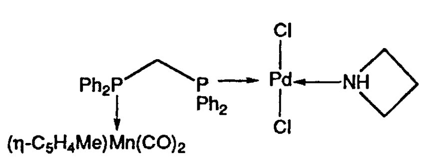

13

Cl atoms, although the anticipated ν(Ru–Cl) absorption around 300–350 cm^{-1} was not observed in the FIR spectrum.[31] Complexes of the type [$RuX_2(CO)_2(PR_3)_2$] are known with an all-*cis*[32] or a *trans,cis,cis* structure.[33] These data are consistent with the structure drawn for **9**.

The reaction of 4 equivalents of complex **1** with [{Ir(cod)(μ-Cl)}$_2$] in toluene gave the new compound [{[(OC)$_2$(η-C_5H_4Me)Mn(μ-dppm)]$_2$Ir(μ-Cl)}$_2$] **10**. Compared to **1**, no significant change was observed for the carbonyl stretches. The ^{31}P-{^{1}H} NMR spectrum is very similar to that of **6**, displaying a quadrupole-broadened singlet at δ 87.9 for the manganese-bound phosphorus atoms and a triplet at δ 14.1 for the iridium-bound phosphorus atoms. As for **6** this resonance can be described as a 'deceptively simple triplet' of an expected AA'XX' pattern with N = 19 Hz. We therefore propose a chloride-bridged structure for **10** similar to that of **6**.

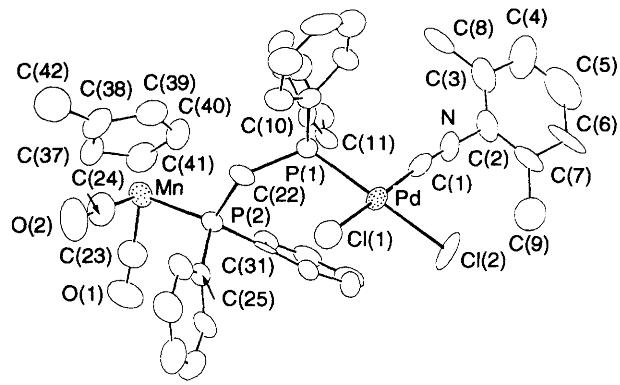

Fig. 3 View of the molecular structure of [(OC)$_2$(η-C_5H_4Me)Mn(μ-dppm)Pd($CNC_6H_3Me_2$-2,6)Cl_2] in **12a**·$CHCl_3$. The H atoms are not shown

The yellow, bimetallic complex [(OC)$_2$(η-C_5H_4Me)Mn(μ-dppm)PdCl(η^3-C_3H_4Me)] **11** was obtained by the reaction of [{Pd(C_3H_4Me)(μ-Cl)}$_2$] with 1 equivalent of **1**. The carbonyl stretches of the Mn(CO)$_2$ fragment were only slightly shifted compared to **1**. The ν(Pd–Cl) vibration was found at 296 cm^{-1} and is close to the value reported for [PdCl(η^3-C_3H_4Me)-(PPh_3)].[34a] A broad singlet and a doublet are observed in the ^{31}P-{^{1}H} NMR spectrum at δ 86.3 and 10.3, respectively, with a ^2J(P–P) coupling of 6 Hz. In the ^{1}H NMR spectrum the allyl group displays dynamic behaviour: its characteristic signals are broad at room temperature and sharpen upon increasing the temperature. The *syn*-protons resonate at δ 2.92 (d) and 2.99 (br) at 323 K. Assignment of the *anti*-protons was not possible due to overlap with the signals for the methylene and η-C_5H_5Me protons. Detailed discussions of the ^{1}H NMR spectra of allylpalladium complexes may be found in refs. 34(*b*)–34(*d*).

Another access to dinuclear Mn–Pd complexes without a metal–metal bond consists in the displacement of a dative Mn→Pd interaction by nucleophiles. Thus, reaction of **3** with 1 equivalent of RNC (R = 2,6-xylyl or Bu^t) was accompanied by an immediate colour change from dark green to yellow. The stable complexes **12a** and **12b** were characterized by analytical and spectroscopic methods. The crystal structure of **12a** (see below, Fig. 3) established the geometry of the complex. The *cis* arrangement of the Pd-bound chloride ligands is indicated in the FIR spectrum by the presence of two absorptions around 330 and 295 cm^{-1}. With the aim of preparing a bimetallic carbene complex,[35] we treated **12a** with a slight excess of azetidine in thf.[36] Orange crystals were produced. A ^{31}P-{^{1}H} NMR analysis of the reaction mixture showed the presence of **1** and a new complex **13**, together with minor amounts of [$PdCl_2$(dppm-*P*,*P*)]. No IR absorption for a co-ordinated or free isocyanide ligand was observed after 1 h reaction time. However, analysis of **13** revealed it to be the azetidine complex [(OC)$_2$(η-C_5H_4Me)Mn(μ-dppm)Pd($NHCH_2CH_2CH_2$)Cl_2], similar to **12a** and **12b** except for the *trans* arrangement of the chloride ligands which was established by X-ray diffraction (see below, Fig. 4).

It is surprising that no carbene complex was isolated since the IR ν(C≡N) frequency of the co-ordinated isocyanide in **12a** is in the range where nucleophilic attack by azetidine should occur

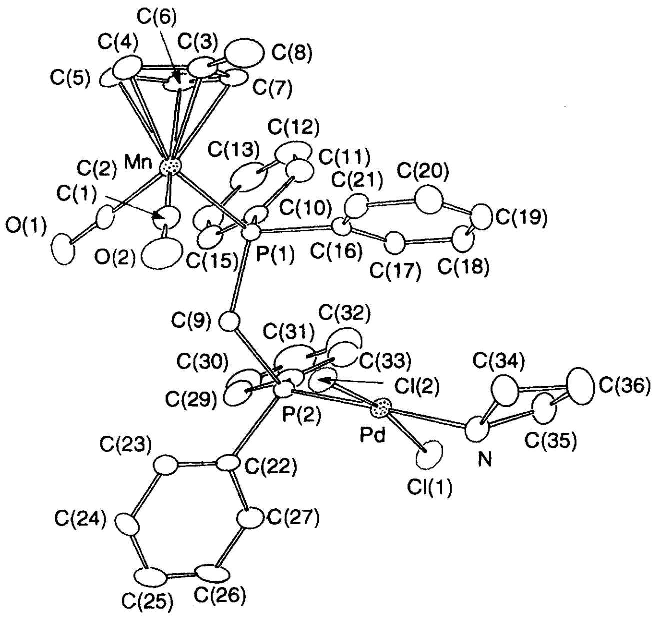

Fig. 4 View of the molecular structure of $[(OC)_2(\eta\text{-}C_5H_4Me)Mn(\mu\text{-dppm})Pd(NHC_3H_6)Cl_2]$ in **13**·$2CH_2Cl_2$. The H atom on N is not shown

to form a carbene complex of type **C**, by extension of previous work on mononuclear palladium complexes.[36] Instead, only replacement of the isocyanide ligand was observed, which is obviously more favourable here than chloride displacement. This reaction occurs with isomerization of the $PdCl_2$ moiety from *cis* to *trans*. When complex **3** was treated with 1 equivalent of azetidine **13** was obtained in higher yield and when a slight excess of azetidine was used some **1** was liberated. This indicates that azetidine reacts with **3** first by displacement of the Mn→Pd bond, followed by that of the isocyanide ligand and then the phosphorus donor **1**.

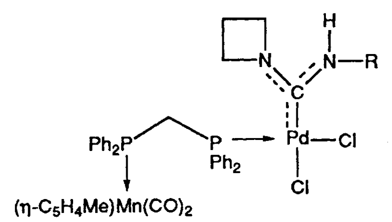

C

Reaction of 1 equivalent of complex **1** with [AuBr(tht)] (tht = tetrahydrothiophene) yielded a new yellow bimetallic complex $[(OC)_2(\eta\text{-}C_5H_4Me)Mn(\mu\text{-dppm})AuBr]$ **14**. The IR absorptions of the $(\eta\text{-}C_5H_4Me)Mn(CO)_2$ fragment are only slightly shifted when compared to **1** (surprisingly towards lower wavenumbers) and a strong ν(Au–Br) absorption was detected at 232 cm^{-1} by FIR spectroscopy.[37] The $^{31}P\text{-}\{^1H\}$ NMR spectrum contains two broadened singlets at δ 87.9 and 23.0, corresponding to the phosphorus atoms bound to manganese and gold, respectively. On lowering the temperature to 253 K the signals split and a $^2J(P\text{–}P)$ coupling of 7 Hz similar to that of **11** was observed. This was interpreted as a temperature-dependent dissociation of the complex.

Reaction of complex **14** with the metalate *mer*-K[Fe{Si(OMe)$_3$}(CO)$_3$(PPh$_3$)][3e] gave the trimetallic complex *mer*-$[(OC)_2(\eta\text{-}C_5H_4Me)Mn(\mu\text{-dppm})AuFe\{Si(OMe)_3\}(CO)_3(PPh_3)]$ **15** in high yields [equation (5)]. The IR spectrum of a toluene solution of **15** in the ν(CO) region consists of the characteristic absorptions of the $AuFe\{Si(OMe)_3\}(CO)_3(PPh_3)$

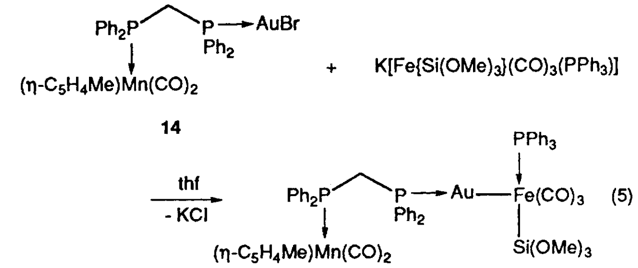

15

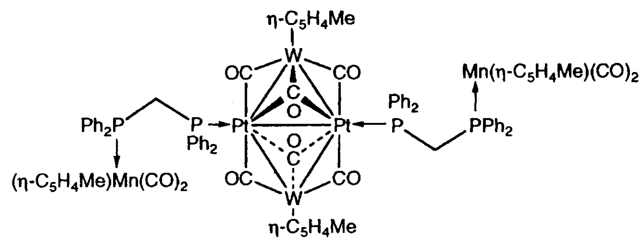

16

fragment at 1974, 1913 and 1887 cm^{-1} [3e] and of the $(\eta\text{-}C_5H_4Me)Mn(CO)_2$ fragment at 1922 and 1859 cm^{-1}. In contrast to **14** the $^{31}P\text{-}\{^1H\}$ NMR spectrum of **15** exhibits three well resolved resonances even at room temperature, indicating that the Au–Fe bond decreases the lability of the complex. These resonances consist of a doublet at δ 82.1 for the manganese-bound phosphorus with a $^2J(P\text{–}P)$ = 16 Hz, a doublet at δ 63.3 for the iron-bound triphenylphosphine, coupled to the gold-bound phosphorus atom with a $^3J(P\text{–}P)$ = 11 Hz and a doublet of doublets at δ 22.2 for the gold-bound phosphorus.

Finally, we examined the possibility of using complex **1** for the construction of new heterometallic clusters. Earlier studies showed the synthetic potential of the chain complexes *trans*-$[Pt\{M(\eta\text{-}C_5H_5)(CO)_3\}_2(NCPh)_2]$ (M = Cr, Mo or W) which react with tertiary phosphine ligands to give heterotetranuclear 'butterfly'-type clusters.[18,22d] The reaction of 1 equivalent of **1** with *trans*-$[Pt\{W(\eta\text{-}C_5H_4Me)(CO)_3\}_2(NCPh)_2]$ in toluene afforded $[Pt_2W_2(\eta\text{-}C_5H_4Me)_2(\mu_3\text{-}CO)_2(\mu\text{-}CO)_4\{(\mu\text{-dppm})Mn(\eta\text{-}C_5H_4Me)(CO)_2\}_2]$ **16** in high yields. Its IR spectrum contains, in addition to the almost unaltered carbonyl vibrations of the $(\eta\text{-}C_5H_4Me)Mn(CO)_2$ fragment, characteristic absorptions of the Pt_2W_2 cluster core at 1738 cm^{-1} for the two μ_3-CO groups, and at 1814 and 1790 cm^{-1} for the four μ-CO groups, similar to those found in $[Pt_2W_2(\eta\text{-}C_5H_5)_2(\mu_3\text{-}CO)_2(\mu\text{-}CO)_4(PPh_3)_2]$.[18b] The $^{31}P\text{-}\{^1H\}$ NMR spectrum displays two multiplets at δ 91.9 and 42.8, corresponding to the manganese- and platinum-bound phosphorus atoms, respectively. This spectrum was analysed in terms of the superimposition of three sub-spectra corresponding to AA'MM', AA'MM'X and AA'MM'XX' (X = X' = ^{195}Pt) spin systems, which allowed the determination of the $^3J(P\text{–}P)$ coupling constant of 117 Hz between the two platinum-bound phosphorus atoms. This value is typical for a linear P–Pt–Pt–P arrangement and therefore indicates a planar Pt_2W_2 core.[18] We have shown previously that bulky phosphines lead to a folding of this core towards tetrahedral which results in a marked decrease of the $^3J(PP)$ coupling constant.[22d] Another rare example of a dppm–Pt–Pt–dppm arrangement was recently found in $[Pt_2(\mu\text{-}S)(\mu\text{-dppm})(dppm\text{-}P)_2]$.[38] Interestingly, the manganese-bound phosphorus atoms display a considerable coupling of 125 Hz to platinum. This contrasts with the situation in **7** or in **4** for P^1, where no $^3J(P\text{–}^{195}Pt)$ was observed for the phosphorus bound to the manganese atom which does not interact with platinum. However, a $^2J(P\text{–}^{195}Pt)$ coupling of 58 Hz was noticed with **4** for the phosphorus associated with a Mn–Pt bond.

In conclusion we have shown that complex **1** is a versatile precursor for the synthesis of polymetallic complexes. It can act as a simple metallophosphine ligand with no involvement of the

Mn in metal–metal bond formation. An intermediate situation was found in the Pt^0 complex **4** with a reversible Pt→Mn bond formation/breaking process whereas a stronger Mn→Pd bond was evidenced in the Pt^{II} complex **3**.

Crystal Structures of Complexes **12a**·$CHCl_3$ *and* **13**·$2CH_2Cl_2$.—The molecular structures are shown in Figs. 3 and 4 and selected distances and angles are given in Tables 1 and 2, respectively. The overall structure of these dinuclear complexes is very much defined by the preferred co-ordination geometries of their metal centres, which are in both cases far apart from each other (6.31 Å in **12a**·$CHCl_3$ and 6.21 Å in **13**·$2CH_2Cl_2$). The P(1)–C(22)–P(2) and P(1)–C(9)–P(2) angles of 126.1(5) and 126.6(6)°, respectively, are characteristic for dppm ligands bridging between two metals not interacting with each other.[29b,39] The (η-C_5H_4Me)Mn(CO)$_2$P fragment has the usual three-legged piano-stool structure, with interligand angles between the carbonyls and the phosphine in the ranges 89.5(4)–93.6(4) (**12a**·$CHCl_3$) and 89.5(6)–92.2(3)° (**13**·$2CH_2Cl_2$), as observed in closely related mononuclear (or homodinuclear) complexes.[9,40] The co-ordination around the palladium atom is square planar, with a *cis* arrangement of the chloride ligands in **12a**·$CHCl_3$, in contrast to the situation in **13**·$2CH_2Cl_2$. The angle between the plane of the C_5H_4Me ligand and the palladium co-ordination plane is 79.4(3)° in **12a**·$CHCl_3$ and 22.4(5)° in **13**·$2CH_2Cl_2$, which reflects the rotational degrees of freedom along the Mn–P–C–P–Pd chain. Accordingly, the angles between the Mn–P(2) and Pd–P(1) vectors in **12a**·$CHCl_3$ and Mn–P(1) and Pd–P(2) in **13**·$2CH_2Cl_2$ amount to 29.8(3) and to 67.3(3)°, respectively. The Pd–Cl distances are significantly different in **12a**·$CHCl_3$ [2.296(3) and 2.342(3) Å], owing to the presence of different *trans* ligands whereas they are comparable in **13**·$2CH_2Cl_2$ [2.289(3) and 2.308(3) Å]. The Pd–P distances compare with those in other dppm complexes of palladium.[2] In **12a**·$CHCl_3$ the four atoms Pd–C(1)–N–C(2) are linearly bonded [175.3(1) and 176(1)°] owing to the presence of the C(1)≡N unit [1.15(2) Å] and the Pd–C(1) distance [1.92(1) Å] is similar to the mean value observed for this bond (1.978 Å).[41] The Pd–N distance of 2.109(9) Å in **13**·$2CH_2Cl_2$ is the same as in the other structurally characterized palladium(II) complex with an azetidine ligand [PdCl(PMe$_2$Ph)(CH$_2$CH$_2$CH$_2$NH){=C(NCH$_2$CH$_2$CH$_2$)NH(C$_6$H$_4$OMe-*p*)}]Cl [2.109(5) Å].[36] The puckering of the azetidine ligand in **13**·$2CH_2Cl_2$ is characterized by a dihedral angle of 19(2)° between the C(34)C(35)N and C(34)C(35)C(36) planes.

Electrochemical Behaviour of [Mn(η-C_5H_4Me)(CO)$_2$(dppm-*P*)] **1** *and its Polymetallic Complexes*.—Fig. 5(*a*) shows the cyclic voltammetric response exhibited by complex **1** in dichloromethane solution, also in comparison with the response of an equimolar amount of [Fe(η-C_5Me_5)$_2$]. The peak-system A/E is due to the well known[42] one-electron oxidation of decamethylferrocene ($E^{\circ\prime} = -0.11$ V), whereas peak B corresponds to the one-electron oxidation of the manganese(I) complex **1**. Clearly, the latter process is followed by relatively fast chemical complications, as evidenced by an $i_{pC}:i_{pB}$ ratio of about 0.2 : 1, as well as by the appearance of peak D. As shown in Fig. 5(*b*), the return peak C is properly detectable only at high scan rates. As a consequence, a lifetime of about 0.5 s can be estimated for the primarily electrogenerated monocation $\mathbf{1}^+$ and an $E^{\circ\prime}$ value of +0.56 V is assigned to the couple $\mathbf{1}$–$\mathbf{1}^+$.

The one-electron nature of the main oxidation process of **1** was deduced from comparison with decamethylferrocene on the cyclic voltammetric time-scale and by controlled-potential coulometry (E_w = +0.7 V) which consumed 1.4 e per molecule, thus indicating that reorganized molecules, in turn oxidizable, form upon decomposition of $\mathbf{1}^+$. Both liquid secondary ion (LSI) and electron impact (EI) mass spectra of the powder obtained from evaporation of the exhaustively electrooxidized solution suggest that the main product is the dinuclear cation [(OC)$_2$(η-C_5H_4Me)Mn{Ph$_2$PCH$_2$P(Ph)CH$_2$PPh$_2$}$_2$Mn(η-C_5H_4Me)(CO)$_2$]$^+$. The LSI spectrum shows a base peak at *m*/*z* 886. The collision-induced dissociation (CID) spectra further confirm the assignment, with the peak at *m*/*z* 886 showing daughter ions at *m*/*z* 809, 732 and 470 respectively, in agreement with the sequential losses of C_6H_5, 2 C_6H_5 and [(η-C_5H_4Me)Mn(CO)$_2$PPh$_2$CH$_2$ + CO], respectively. The fact that the complex resulting from the oxidation process is silent to EI mass spectrometry, in contrast to the parent neutral species, supports its positive charge.

Table 1 Selected bond distances (Å) and angles (°) for [(OC)$_2$(η-C_5H_4Me)Mn(μ-dppm)Pd(CNC$_6$H$_3$Me$_2$-2,6)Cl$_2$]·$CHCl_3$ **12a**·$CHCl_3$

Pd–Cl(1)	2.296(3)	Mn–C(41)	2.12(1)
Pd–Cl(2)	2.342(3)	P(1)–C(10)	1.81(1)
Pd–P(1)	2.262(3)	P(1)–C(16)	1.81(1)
Pd–C(1)	1.92(1)	P(1)–C(22)	1.85(1)
Mn–P(2)	2.229(3)	P(2)–C(22)	1.86(1)
Mn–C(23)	1.74(1)	P(2)–C(25)	1.81(1)
Mn–C(24)	1.76(1)	P(2)–C(31)	1.84(1)
Mn–C(37)	2.15(1)	C(1)–N	1.15(2)
Mn–C(38)	2.16(1)	N–C(2)	1.39(2)
Mn–C(39)	2.15(1)	C(23)–O(1)	1.18(2)
Mn–C(40)	2.14(1)	C(24)–O(2)	1.16(2)
C(1)–Pd–P(1)	94.1(3)	C(22)–P(1)–Pd	118.3(3)
C(1)–Pd–Cl(1)	174.6(3)	P(1)–C(22)–P(2)	126.1(5)
C(1)–Pd–Cl(2)	87.1(3)	C(23)–Mn–C(24)	91.9(6)
P(1)–Pd–Cl(1)	86.8(1)	C(23)–Mn–P(2)	89.5(4)
P(1)–Pd–Cl(2)	177.9(1)	C(24)–Mn–P(2)	93.6(4)
Cl(1)–Pd–Cl(2)	91.7(1)	O(1)–C(23)–Mn	177(1)
N–C(1)–Pd	175.3(1)	O(2)–C(24)–Mn	177(1)
C(1)–N–C(2)	176(1)	C(25)–P(2)–C(31)	100.9(5)
C(10)–P(1)–C(16)	106.0(5)	C(25)–P(2)–C(22)	101.1(4)
C(10)–P(1)–C(22)	105.8(4)	C(25)–P(2)–Mn	112.1(3)
C(10)–P(1)–Pd	115.5(3)	C(31)–P(2)–C(22)	104.9(4)
C(16)–P(1)–C(22)	104.4(5)	C(31)–P(2)–Mn	120.3(3)
C(16)–P(1)–Pd	105.5(3)	C(22)–P(2)–Mn	114.8(3)

Numbers in parentheses are estimated standard deviations (e.s.d.s) in the least significant digits.

Table 2 Selected bond distances (Å) and angles (°) for [(OC)$_2$(η-C_5H_4Me)Mn(μ-dppm)Pd(NHC$_3$H$_6$)Cl$_2$]·$2CH_2Cl_2$ **13**·$2CH_2Cl_2$

Pd–Cl(1)	2.289(3)	P(1)–C(9)	1.85(1)
Pd–Cl(2)	2.308(3)	P(1)–C(10)	1.82(1)
Pd–P(2)	2.256(3)	P(1)–C(16)	1.83(1)
Pd–N	2.11(1)	P(2)–C(9)	1.82(1)
Mn–P(1)	2.218(3)	P(2)–C(22)	1.83(1)
Mn–C(1)	1.75(1)	P(2)–C(28)	1.82(1)
Mn–C(2)	1.75(2)	C(1)–O(1)	1.14(1)
Mn–C(3)	2.17(1)	C(2)–O(2)	1.16(2)
Mn–C(4)	2.14(1)	N–C(34)	1.50(2)
Mn–C(5)	2.15(1)	N–C(35)	1.48(2)
Mn–C(6)	2.14(1)	N–C(36)	2.13(2)
Mn–C(7)	2.15(1)	C(34)–C(36)	1.50(2)
		C(35)–C(36)	1.49(2)
Cl(1)–Pd–Cl(2)	168.6(1)	C(9)–P(1)–C(16)	104.9(5)
Cl(1)–Pd–P(2)	92.9(1)	C(10)–P(1)–C(16)	105.3(6)
Cl(1)–Pd–N	86.7(3)	C(9)–P(2)–C(22)	102.7(5)
Cl(2)–Pd–P(2)	89.1(1)	C(9)–P(2)–C(28)	105.5(5)
Cl(2)–Pd–N	91.1(3)	C(22)–P(2)–C(28)	103.2(6)
P(2)–Pd–N	179.0(3)	Mn–C(1)–O(1)	180(1)
P(1)–Mn–C(1)	90.8(4)	Mn–C(2)–O(2)	178(1)
P(1)–Mn–C(2)	92.2(4)	P(1)–C(9)–P(2)	126.6(6)
P(1)–Mn–C(3)	118.4(4)	Pd–N–C(34)	124.0(8)
P(1)–Mn–C(4)	154.7(4)	Pd–N–C(35)	119.5(8)
P(1)–Mn–C(5)	135.2(5)	C(34)–N–C(35)	88(1)
P(1)–Mn–C(6)	99.4(4)	N–C(34)–C(36)	90(1)
P(1)–Mn–C(7)	90.8(4)	N–C(35)–C(36)	91(1)
C(1)–Mn–C(2)	89.7(6)	C(34)–C(36)–C(35)	87(1)
C(9)–P(1)–C(10)	106.0(5)		

Numbers in parentheses are e.s.d.s in the least significant digits.

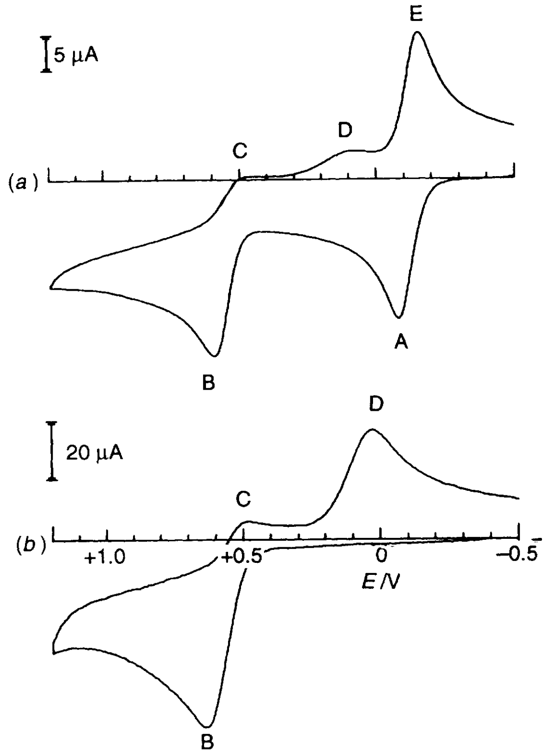

Fig. 5 Cyclic voltammograms recorded at a platinum electrode on a CH_2Cl_2 solution containing $[NBu_4][ClO_4]$ (0.2 mol dm^{-3}) and (*a*) complex **1** (8.0 × 10^{-4} mol dm^{-3}) and $[Fe(\eta\text{-}C_5Me_5)_2]$ (9.0 × 10^{-4} mol dm^{-3}), scan rate 0.2 V s^{-1}, and (*b*) **1** (8.0 × 10^{-4} mol dm^{-3}), scan rate 2 V s^{-1}

Under the same experimental conditions, dppm undergoes an irreversible oxidation at E_p = +1.29 V. It is relevant that $[Mn(\eta\text{-}C_5H_4Me)(CO)_2(PPh_3)]$ [10a,b] or $[Mn(\eta\text{-}C_5H_5)(CO)_2(PPh_3)]$ [10a,c] undergoes reversible oxidation to the corresponding monocation. The corresponding redox potentials are summarized in Table 3.

Fig. 6 shows the cyclic voltammetric response exhibited by the dimanganese complex $[(OC)_2(\eta\text{-}C_5H_4Me)Mn(\mu\text{-}dppm)Mn(\eta\text{-}C_5H_4Me)(CO)_2]$ **2**. Now, the Mn^I–Mn^{II} oxidation of the parent precursor **1** (peak system A/D, $E^{o\prime}$ = +0.56 V) increases its extent of chemical reversibility and is followed by the one-electron oxidation of the coupled manganese(I) fragment (peak system B/C, $E^{o\prime}$ = +0.65 V). Also in this case, chemical complications accompany the two sequential electron removals, in that 3.1 e per molecule are consumed in controlled-potential coulometry (E_w = +0.75 V), as also preliminarily pointed out by the presence of peak E in the reverse scan. The appearance of two closely spaced, but distinct oxidation processes clearly indicates that the dppm bridging ligand permits electronic communication between the two manganese centres.[43] The strictly related complex $[(OC)_2(\eta\text{-}C_5H_5)Mn(\mu\text{-}dppm)Mn(\eta\text{-}C_5H_5)(CO)_2]$ also exhibits two sequential one-electron oxidations with features of chemical reversibility.[10c]

As easily deduced from Fig. 7, the heterobinuclear complex $[(OC)_2(\eta\text{-}C_5H_4Me)Mn(\mu\text{-}dppm)AuBr]$ **14** displays the one-electron oxidation of the manganese(I) moiety and an irreversible reduction (E_p = −1.72 V) likely centred on the gold(I) fragment. In confirmation that co-ordination of the second pendant diphenylphosphino group of the diphosphine kinetically stabilizes the 18/17-electron redox change, the oxidation process displays a good extent of chemical reversibility ($i_{pc}:i_{pa}$ = 0.6:1 at 0.2 V s^{-1}). In addition, co-ordination to the gold fragment thermodynamically stabilizes the 18-electron manganese(I) complex in that the Mn^I–Mn^{II} electron removal is made slightly more difficult ($E^{o\prime}$ = 0.62 V).

Table 3 Formal electrode potentials (in V, *vs.* SCE) for the one-electron oxidation of complexes of the type $[Mn(\eta\text{-}C_5R_5)(CO)_2(phosphine)]$

Complex	$E^{o\prime}_{0/+}$	Solvent	Ref.
$[Mn(\eta\text{-}C_5H_5)(CO)_2(PPh_3)]$	+0.52	CH_2Cl_2	10(*a*)
	+0.68	CH_2Cl_2	10(*c*)
$[Mn(\eta\text{-}C_5H_4Me)(CO)_2(PPh_3)]$	+0.51	CH_2Cl_2	10(*a*)
	+0.52	MeCN	10(*b*)
	+0.52	Me_2CO	10(*b*)
$[Mn(\eta\text{-}C_5Me_5)(CO)_2(PPh_3)]$	+0.30	CH_2Cl_2	10(*a*)
$[Mn(\eta\text{-}C_5H_4Me)(CO)_2(dppm\text{-}P)]$	+0.56*	CH_2Cl_2	This work

* Coupled to chemical complications.

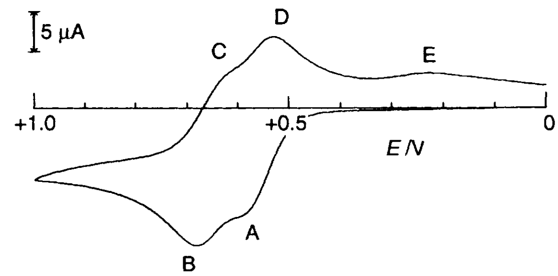

Fig. 6 Cyclic voltammogram recorded at a platinum electrode of a CH_2Cl_2 solution of complex **2** (9.0 × 10^{-4} mol dm^{-3}) and $[NBu_4][ClO_4]$ (0.2 mol dm^{-3}). Scan rate 0.1 V s^{-1}

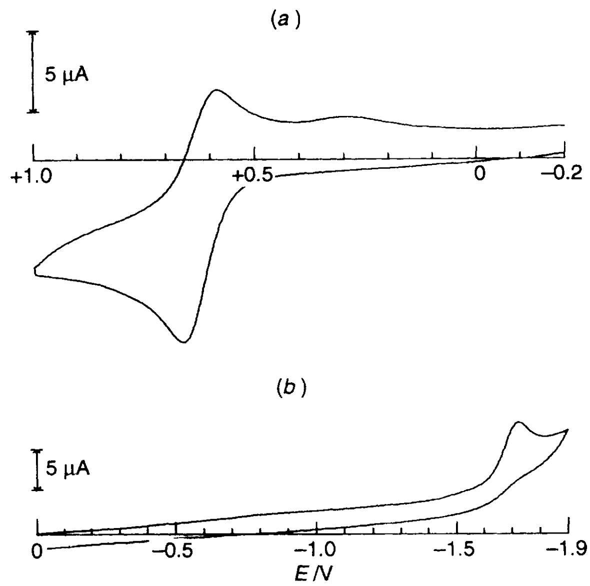

Fig. 7 Cyclic voltammograms recorded at a platinum electrode of a CH_2Cl_2 solution of complex **14** (7.0 × 10^{-4} mol dm^{-3}) and $[NBu_4][ClO_4]$ (0.2 mol dm^{-3}). Scan rate 0.2 V s^{-1}

A qualitatively similar response is exhibited by the heterobinuclear complex **3**. In agreement with the electron donation from manganese to palladium, the one-electron oxidation of the manganese centre is significantly more difficult ($E^{o\prime}$ = +0.98 V). Co-ordination of the pendant diphenylphosphino groups imparts features of transient chemical reversibility ($i_{pc}:i_{pa}$ = 0.5:1 at 0.2 V s^{-1}). An irreversible reduction, confidently attributable to the palladium(II) fragment, is also present (E_p = −0.77 V).

The redox behaviour of the trinuclear complex **7** is shown in Fig. 8. In addition to the irreversible reduction at E_p = −1.57 V, which can be confidently assigned to the Pt^{II}–Pt^0 step, commonly exhibited by platinum(II) complexes, the most significant feature is the appearance of the single two-electron

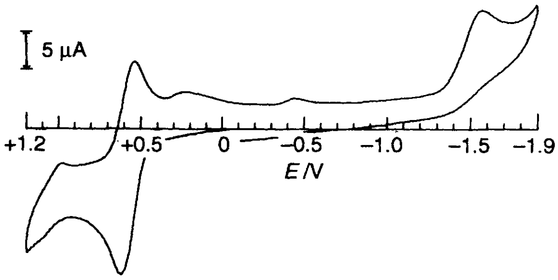

Fig. 8 Cyclic voltammogram recorded at a platinum electrode on a CH_2Cl_2 solution containing complex **7** (5.3×10^{-4} mol dm^{-3}) and $[NBu_4][ClO_4]$ (0.2 mol dm^{-3}). Scan rate 0.2 V s^{-1}

oxidation wave at $E^{o\prime} = +0.58$ V (2.0 e per molecule in controlled-potential coulometry, $E_w = +0.7$ V). The concomitant oxidation of the two manganese(I) centres, which displays a good extent of chemical reversibility (at 0.2 V s^{-1}, $i_{pc}:i_{pa} = 0.7:1$), clearly reveals that the central $PtCl_2$ unit does not permit electronic interaction between the two manganese(I) appendices.

The electrochemical behaviour of the tetranuclear Mn_2Rh_2 complex **5** is rather complicated. As illustrated in Fig. 9(*a*), there is a rich series of oxidation steps. In addition, an irreversible multielectron reduction process (not shown) is present at $E_p = -1.85$ V. Because of the good chemical reversibility of the first two steps ($E^{o\prime}_{0/+} = +0.17$ V, $E^{o\prime}_{+/2+} = +0.39$ V), Fig. 9(*b*), we tentatively assign them to the one-electron oxidation of the two manganese(I) centres. Also in this case, such electron removals are coupled to chemical complications, in that controlled-potential coulometry at the first step ($E_w = +0.2$ V) consumes 1.5 per molecule. Provided this assignment is correct, we must conclude that: (*i*) based on the significantly easier access to the oxidized states, electron density must be poured into the manganese fragments by the rhodium units; (*ii*) the relatively large separation in the redox potentials ($\Delta E = 0.22$ V) should testify to a relatively extended interaction between the two manganese moieties.

Finally, Fig. 10 shows the simple, but difficult to interpret, cyclic voltammetric profile exhibited by the hexanuclear $Mn_2Pt_2W_2$ complex **16**. Two irreversible multielectron processes are displayed: (*i*) one oxidation process at $E_p = +0.86$ V, which exhibits, in the reverse scan, a decomposition reduction peak at $E_p = -0.67$ V; (*ii*) one reduction process at $E_p = -1.45$ V, which exhibits, in the reverse scan, a decomposition oxidation peak at $E_p = -0.18$ V. Both the decomposition peaks do not display directly associated responses in the reverse scan. As a proof of the complex redox pattern, controlled-potential coulometry at the potentials of the reduction process ($E_w = -1.5$ V) consumes 9.3 e per molecule. We note that the reduction process is quite reminiscent of that found in $[Pt_2W_2(\eta\text{-}C_5H_5)_2(CO)_6(PPh_3)_2]$,[44] which is a good model for the central tetrametal unit of **16**, whereas its easy, reversible oxidation steps are absent here.

Experimental

All experiments were carried out using Schlenk-tube techniques, under oxygen-free nitrogen. Elemental analyses were performed by the Service Central de Microanalyses du CNRS. Infrared spectra were obtained using a Bruker IFS 66/113 (FTIR) spectrometer, and NMR spectra on Bruker SY200 and AC300P instruments with proton chemical shifts measured relative to tetramethylsilane and phosphorus chemical shifts relative to phosphoric acid (external reference) with downfield chemical shifts reported as positive. FAB Mass spectra were measured on a Fisons ZAB-HF spectrometer (Université Louis Pasteur, R. Hueber). Material and apparatus for electrochemistry[45] and related mass spectrometric studies[46] have been described elsewhere. Under the experimental conditions used,

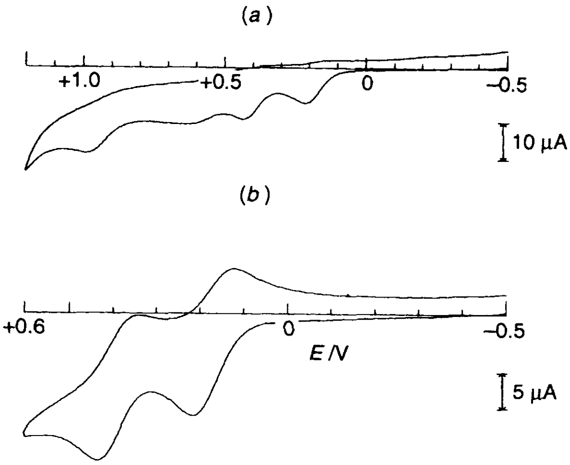

Fig. 9 Cyclic voltammograms recorded at a platinum electrode of a CH_2Cl_2 solution of complex **5** (7.4×10^{-4} mol dm^{-3}) and $[NBu_4][ClO_4]$ (0.2 mol dm^{-3}). Scan rate: (*a*) 0.2, (*b*) 0.5 V s^{-1}

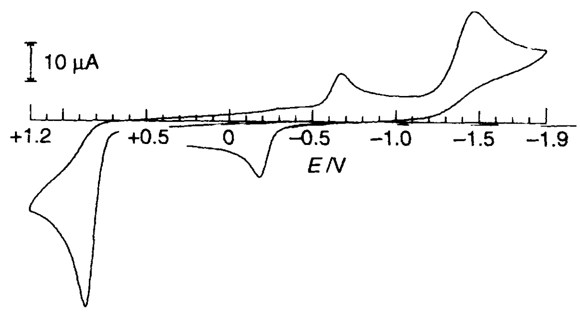

Fig. 10 Cyclic voltammogram recorded at a platinum electrode of a CH_2Cl_2 solution of complex **16** (5.0×10^{-4} mol dm^{-3}) and $[NBu_4][ClO_4]$ (0.2 mol dm^{-3}). Scan rate 0.2 V s^{-1}

the ferrocene–ferrocenium couple used for calibration was located at +0.44 V *vs.* SCE.

The reactions were generally monitored by IR spectroscopy in the ν(CO) region. Photochemical reactions were performed in an irradiation vessel using a water- or methanol-cooled high-pressure mercury lamp (180 W, TQ 150, Heraeus). Unless otherwise specified the pure complexes are air-stable in the solid state for prolonged periods of time. The complexes $[Pt(cod)_2]$,[47] $[\{Pd(\eta^3\text{-}C_3H_4Me)(\mu\text{-}Cl)\}_2]$,[48] $[\{Re(CO)_3thf(\mu\text{-}Br)\}_2]$,[49] $[\{RuCl(CO)_3(\mu\text{-}Cl)\}_2]$,[50] $[\{Rh(cod)(\mu\text{-}Cl)\}_2]$,[51] $[AuBr(tht)]$ (tht = tetrahydrothiophene),[52] $K[Fe\{Si(OMe)_3\}(CO)_3(PPh_3)]$[3e] and *trans*-$[Pt\{W(\eta\text{-}C_5H_4Me)(CO)_3\}_2(NCPh)_2]$[18b] were prepared according to literature methods.

Synthesis of the Complexes.—$[Mn(\eta\text{-}C_5H_4Me)(CO)_2(dppm\text{-}P)]$ **1**. A solution of $[Mn(\eta\text{-}C_5H_4Me)(CO)_3]$ (1.65 cm^3, 10 mmol) in thf (600 cm^3) was irradiated at −10 °C for 4–5 h. Irradiation was stopped when the ν(CO) absorption of $[Mn(\eta\text{-}C_5H_4Me)(CO)_3]$ had nearly completely disappeared. The resulting deep red solution of $[Mn(\eta\text{-}C_5H_4Me)(CO)_2(thf)]$ [IR (thf): ν(CO) 1923vs and 1847vs cm^{-1}] was kept cold and was added over 2 h to a stirred solution of dppm (4.00 g, 10.4 mmol) in thf (50 cm^3). The reaction mixture was stirred overnight and then evaporated under reduced pressure. The resulting orange oil was vigorously stirred with hexane (*ca.* 100 cm^3) until a suspension resulted. The solid was filtered off, washed once with cold hexane and dried *in vacuo* yielding 5 g of a yellow powder consisting mainly of complex **1** and $[\{Mn(\eta\text{-}C_5H_4Me)(CO)_2\}_2(\mu\text{-}dppm)]$ **2**. The crude product was dissolved in diethyl ether (20 cm^3) and mixed with SiO_2 (10 g). After evaporation of the ether the resulting powder was placed on a chromatography column (5 × 50 cm, <230 mesh SiO_2). Elution with hexane–ether (9:1) at 300 cm^3 h^{-1} 2–3 bar (bar =

10^5 Pa) yielded first unreacted dppm, then some remaining [Mn(η-C_5H_4Me)$(CO)_3$] (R_f = 0.6), followed by the products **1** (R_f = 0.3) and **2** (R_f = 0.2). The fraction containing **1** was evaporated until the beginning of precipitation. Crystallization overnight at −30 °C yielded the bright yellow, microcrystalline and air-stable **1** {1.60 g, 30% based on [Mn(η-C_5H_4Me)$(CO)_3$]} (Found: C, 69.05; H, 4.95. Calc. for $C_{33}H_{29}MnO_2P_2$: C, 69.00; H, 5.10%). IR (CH_2Cl_2): ν(CO) 1925vs and 1859vs; (KBr) 1923vs and 1856vs cm^{-1}. FIR (polyethylene): 394w, 382w, 372m, 352mw and 320mw cm^{-1}. NMR: ^1H(200 MHz, $CDCl_3$), δ 1.66 (s, 3 H, CH_3), 3.27 [d, 2 H, CH_2, ^2J(P–H) = 7.1], 3.91 (m, 4 H, C_5H_4) and 6.95–7.58 (m, 20 H, C_6H_5); ^{31}P-{^1H} (81.02 MHz, CH_2Cl_2–C_6D_6), δ 85.5 [br d, P(Mn), ^2J(P–P) = 77 Hz] and −26.3 (d, unco-ordinated P).

[{Mn(η-C_5H_4Me)$(CO)_2$}$_2$(μ-dppm)] **2**. This was prepared as described above. The corresponding fraction collected during chromatography was evaporated until the beginning of precipitation. Standing overnight at −30 °C yielded yellow, microcrystalline complex **2** {0.70 g, 20% based on [Mn(η-C_5H_4Me)$(CO)_3$]} (Found: C, 64.80; H, 4.70. Calc. for $C_{41}H_{36}Mn_2O_4P_2$: C, 64.40; H, 4.75%). IR (KBr): ν(CO) 1923vs and 1856vs cm^{-1}. FIR (polyethylene): 373s, 363ms, 339s, 329ms and 258w cm^{-1}. NMR: ^1H(200 MHz, $CDCl_3$), δ 1.69 (s, 6 H, CH_3), 3.64 (br, 2 H, CH_2), 3.77 (br, 4 H, C_5H_4), 3.90 (br, 4 H, C_5H_4) and 7.30–7.41 (m, 20 H, C_6H_5); ^{31}P-{^1H} (81.02 MHz, CH_2Cl_2–C_6D_6), δ 88.5 [br s, P(Mn)].

[$(OC)_2$(η-C_5H_4Me)Mn(μ-dppm)PdCl_2] **3**. Solid complex **1** (0.258 g, 0.450 mmol) was added in three portions to a solution of [$PdCl_2(NCPh)_2$] (0.182 g, 0.50 mmol) in toluene (20 cm^3). An immediate colour change to dark brown was observed and a dark solid precipitated. After stirring for 0.2 h the solid was filtered from the bright green solution and washed with toluene. The residue was extracted with CH_2Cl_2 and the solution was filtered. Precipitation with hexane yielded a dark green powder (0.24 g, 58%) (Found: C, 45.25; H, 3.25. Calc. for $C_{33}H_{29}Cl_2MnO_2P_2Pd{\cdot}2CH_2Cl_2$: C, 45.60; H, 3.60%). IR (CH_2Cl_2): ν(CO) 1896w and 1849s; (KBr) 1896w and 1850s cm^{-1}. FIR (polyethylene): ν(Pd–Cl) 299s and 282s cm^{-1}. NMR: ^1H(200 MHz, $CDCl_3$), δ 1.78 (s, 3 H, CH_3), 2.91 [dd, 2 H, CH_2, ^2J(H–P) = 11.8, 9.7], 4.36 (m, 2 H, C_5H_4), 4.63 (m, 2 H, C_5H_4) and 7.20–7.64 (m, 20 H, C_6H_5); ^{31}P-{^1H} [81.02 MHz, CH_2Cl_2–$(CD_3)_2CO$], δ 89.8 [br d, P(Mn)] and 40.5 [d, ^{2+3}J(P–P) = 61 Hz, P(Pd)].

[Pt{(μ-dppm)Mn(η-C_5H_4Me)$(CO)_2$}$_2$] **4**. Solid complex **1** (0.100 g, 0.17 mmol) and [Pt$(cod)_2$] (0.038 g, 0.09 mmol) were mixed and toluene (5 cm^3) was added. The mixture was stirred for 1 h and the resulting orange solution was filtered and the solvent removed under vacuum. The residue was dissolved in CH_2Cl_2 (1 cm^3) and hexane (10 cm^3). The volume was reduced to 5 cm^3 and the solution was left at −30 °C for 24 h to yield orange microcrystals (0.10 g, 80%) (Found: C, 57.60; H, 4.50. Calc. for $C_{66}H_{58}Mn_2O_4P_4Pt{\cdot}0.5CH_2Cl_2$: C, 57.60; H, 4.30%). IR (KBr): ν(CO) 1922s, 1856 (br) s and 1682mw (br) cm^{-1}. FIR (polyethylene): 343s, 229m and 121s cm^{-1}. NMR: ^1H(200 MHz, CD_2Cl_2, 233 K), δ 1.57 (s, 3 H, CH_3), 1.69 (s, 3 H, CH_3), 3.14–4.12 (m, 8 H, CH_2, C_5H_4, resonances poorly resolved) and 5.86–7.59 (m, 40 H, C_6H_5); ^{31}P-{^1H} (81.02 MHz, toluene–C_6D_6, 305 K), δ 81.9 [br, P(Mn)] and *ca.* 50 to −10 [vbr, P(Pt)]; (253 K) δ 83.3 [d, P^1(Mn), $^2J(P^1–P^3)$ = 13.1], 71.6 [dd, P^2(Mn), $^{2+3}J(P^2–P^4)$ = 112.6, $^{3+4}J(P^2–P^3)$ = 50.2, $^2J(P^2–^{195}Pt)$ = 57.8], 40.7 [ddd, P^3(Pt), $^2J(P^3–P^1)$ = 13.1, $^2J(P^3–P^4)$ = 57.0, $^{3+4}J(P^3–P^2)$ = 50.2, $^1J(P^3–^{195}Pt)$ = 4367] and −1.6 [dd, P^4(Pt), $^{2+3}J(P^4–P^2)$ = 112.6, $^2J(P^4–P^3)$ = 57.0, $^1J(P^4–^{195}Pt)$ = 2703 Hz (by spectral simulation)].

[{(η-C_5H_4Me)Mn(μ-CO)$_2$(μ-dppm)Rh(μ-Cl)}$_2$] **5**. Solid complex **1** (0.233 g, 0.405 mmol) and [{Rh(cod)(μ-Cl)}$_2$] (0.100 g, 0.202 mmol) were mixed and toluene (5 cm^3) was added. The mixture was stirred for 6 h and the resulting deep green solution filtered and evaporated to 2 cm^3. Slow diffusion of hexane into the solution yielded green crystals (0.15 g, 77%) (Found: C, 55.50; H, 4.05. Calc. for $C_{66}H_{58}Cl_2Mn_2O_4P_4Rh_2$: C, 55.60; H, 4.10%). FAB$^+$ mass spectrum (*m*-$O_2NC_6H_4$–CH_2OH, thf): *m*/*z* 1367.7, [*M* − 2CO]$^+$; 1298.8, [*M* − 2CO − 2Cl + H]$^+$; 1270.9 (1298.8 − CO); 1242.9 (1298.8 − 2CO); 1135.9, [*M* − 2Cl − Mn(η-C_5H_4Me)$(CO)_2$ − CO]$^+$; and 1108.9 (1135.9 − CO). IR (CH_2Cl_2): ν(CO) 1783w and 1750vs; (KBr) 1783w, 1748s and 1739 (sh) cm^{-1}. FIR (polyethylene): 377w, 349m, 322w, 286 (sh), 278 (sh) m, 264s and 255s cm^{-1}. NMR: ^1H(200 MHz, CD_2Cl_2), δ 1.56 (s, 6 H, CH_3), 2.28 [t, 4 H, CH_2, ^2J(H–P) = 11.2], 3.50 (m, 4 H, C_5H_4), 3.96 (m, 4 H, C_5H_4) and 7.17–7.64 (m, 40 H, C_6H_5); ^{31}P-{^1H} (81.02 MHz, CH_2Cl_2–CD_2Cl_2), δ 94.7 [br d, P(Mn), ^{2+3}J(P–P) = 77] and 52.4 [ddd, P(Rh), ^1J(P–Rh) = 164, ^4J(P–P) = 2 Hz].

[{[$(OC)_2$(η-C_5H_4Me)Mn(μ-dppm)]$_2$Rh(μ-Cl)}$_2$] **6**. Solid complex **1** (0.115 g, 0.20 mmol) and [{Rh(cod)(μ-Cl)}$_2$] (0.025 g, 0.05 mmol) were mixed and toluene (5 cm^3) was added. The mixture was stirred for 5 d. A dark green solution resulted with a bright green precipitate (the colour of **6** might be perturbed by that of the intermediate **5**). The solid was filtered off, washed with hexane (0.075 g, 55%) and dissolved in CH_2Cl_2. This solution was used for recording the ^{31}P-{^1H} spectrum (81.02 MHz, CH_2Cl_2–C_6D_6): δ 87.1 [br s, P(Mn)] and 21.2 [dt, P(Rh), ^1J(P–Rh) = 126, *N* = 14 Hz].

[$PtCl_2${(μ-dppm)Mn(η-C_5H_4Me)$(CO)_2$}$_2$] **7**. Solid complex **1** (0.100 g, 0.174 mmol) and [$PtCl_2(NCPh)_2$] (0.031 g, 0.085 mmol) were mixed and toluene (5 cm^3) was added. The mixture was stirred for 1 h and the resulting clear yellow solution was filtered, evaporated to 1 cm^3 and hexane (10 cm^3) was added. The mixture was left at −30 °C for 24 h and the resulting microcrystalline precipitate filtered off and washed with cold hexane (0.118 g, 92%) (Found: C, 57.95; H, 4.35. Calc. for $C_{66}H_{58}Cl_2Mn_2O_4P_4Pt{\cdot}C_6H_5CH_3$: C, 58.20; H, 4.40%). IR (CH_2Cl_2): ν(CO) 1925s and 1858s; (KBr) 1928 (sh), 1922vs, 1909m (sh), 1858vs (br) and 1842m cm^{-1}. FIR (polyethylene): 377m, 357m and 340s cm^{-1}. NMR: ^1H(200 MHz, CD_2Cl_2), δ 1.72 (s, 6 H, CH_3), 3.8–4.0 (overlapping signals, 12 H, CH_2, C_5H_4) and 7.05–7.48 (m, 40 H, C_6H_5); (C_6D_6), δ 1.62 (s, 6 H, CH_3), 3.96 (m, 4 H, C_5H_4), 4.02 (m, 4 H, C_5H_4), 4.38 (m, 4 H, CH_2) and 6.88–7.71 (m, 40 H, C_6H_5); ^{31}P-{^1H} (81.02 MHz, CH_2Cl_2–C_6D_6), δ 88.4 [br, P(Mn)] and 6.6 [AA′ part of an AA′XX′ spin system, P(Pt), $^1J(P–^{195}Pt)$ = 2579, *N* = 23 Hz].

[ReBr$(CO)_3${(μ-dppm)Mn(η-C_5H_4Me)$(CO)_2$}$_2$] **8**. The preparation and work-up were similar to those for complex **7**, using **1** (0.100 g, 0.174 mmol) and [{Re$(CO)_3$(thf)(μ-Br)}$_2$] (0.037 g, 0.0435 mmol), yield 0.11 g (85%). Complex **8** tends to precipitate as an oily residue upon addition of hexane. FAB$^+$ mass spectrum (*m*-$O_2NC_6H_4CH_2OH$, toluene): *m*/*z* 1498.0/1499.0, *M*$^+$, [*M* + H]$^+$; 1442.0, [*M* − 2CO]$^+$; 1419.1, [*M* − Br]$^+$; 1229.1, [*M* − Br − Mn(η-C_5H_4Me)$(CO)_2$]$^+$; 1201.1 (1229 − CO); 1039.1, [*M* − Br − 2[Mn($η^5$-C_5H_4Me)-$(CO)_2$]$^+$; 1011.1 (1039 − CO); 983.1 (1039 − 2CO); and 817.0 (1229 − dppm − CO). IR (KBr): ν(CO) 2025s, 1940 (sh) m and 1907m [Re$(CO)_3$]; 1925vs and 1860vs cm^{-1} [Mn$(CO)_2$]. FIR (polyethylene): 347m, 337m, 332m, 276m and 260m; ν(Re–Br) 186m cm^{-1}. NMR: ^1H(200 MHz, $CDCl_3$), δ 1.71 (s, 6 H, CH_3), 3.72–4.05 (overlapping signals, 12 H, CH_2, C_5H_4) and 6.93–7.55 (m, 40 H, C_6H_5); ^{31}P-{^1H} (81.02 MHz, CH_2Cl_2–C_6D_6), δ 91.0 [br m, P^1(Mn), P^2(Mn)] and −3.9 [m, AA′XX′ spin system, P^3(Re), P^4(Re), $J(P^1–P^3)$ = −0.5, $J(P^1–P^4)$ = 31.0, $J(P^2–P^3)$ = 31.6, $J(P^2–P^4)$ = −1.1, $J(P^3–P^4)$ = 26.2 Hz (data from spectral simulation)].

[$RuCl_2(CO)_2${(μ-dppm)Mn(η-C_5H_4Me)$(CO)_2$}$_2$] **9**. The preparation and work-up were similar to those of complex **7**, using **1** (0.100 g, 0.174 mmol) and [{RuCl$(CO)_3$(μ-Cl)}$_2$] (0.022 g, 0.0435 mmol), yield 0.105 g, 90%. IR (KBr): ν(CO) 2055s, 1991s, 1925vs and 1858vs cm^{-1}. FIR (polyethylene): 351m, 303m and 279m (br) cm^{-1}. NMR: ^1H(200 MHz, $CDCl_3$), δ 1.81 (s, 6 H, CH_3), 4.03, 4.10 (m, 8 H, C_5H_4), 4.69 (m, 4 H, CH_2) and 7.09–7.68 (m, 40 H, C_6H_5); ^{31}P-{^1H} (81.02 MHz, CH_2Cl_2–C_6D_6), δ 89.8 [AA′XX′ spin system, br, P(Mn)] and 17.7 [AA′XX′ spin system, P(Ru), *N* = 34 Hz].

[{[(OC)$_2$(η-C$_5$H$_4$Me)Mn(μ-dppm)]$_2$Ir(μ-Cl)}$_2$] **10**. The preparation and work-up were similar to those of complex **7**, using **1** (0.100 g, 0.174 mmol) and [{Ir(cod)(μ-Cl)}$_2$] (0.029 g, 0.0435 mmol). IR (KBr): ν(CO) 1927vs and 1851vs cm^{-1}. NMR: ^{1}H(200 MHz, CDCl$_3$), δ 1.71 (s, 6 H, CH$_3$), 4.00, 4.15 (m, 12 H, C$_5$H$_4$, CH$_2$) and 7.1–7.6 (m, 40 H, C$_6$H$_5$); ^{31}P-{^{1}H} (81.02 MHz, CH$_2$Cl$_2$–C$_6$D$_6$), δ 87.9 [s, br, P(Mn)] and 14.1 [AA'XX' spin system, P(Ir), N = 19 Hz].

[(OC)$_2$(η-C$_5$H$_4$Me)Mn(μ-dppm)PdCl(η^3-C$_3$H$_4$Me)] **11**. The preparation and work-up were similar to those of complex **7**, using **1** (0.100 g, 0.174 mmol), [{Pd(η^3-C$_3$H$_4$Me)(μ-Cl)}$_2$] (0.030 g, 0.087 mmol), yield 0.10 g, 80% (Found: C, 57.65; H, 4.70. Calc. for C$_{37}$H$_{36}$ClMnO$_2$P$_2$Pd: C, 57.60; H, 4.70%). IR (CH$_2$Cl$_2$): ν(CO) 1923s and 1856s cm^{-1}. FIR (polyethylene): 388m and 356s; ν(Pd–Cl) 296s cm^{-1}. NMR: ^{1}H(200 MHz, CDCl$_3$, 323 K), 1.59 (s, 3 H, CH$_3$), 1.71 (s, 3 H, CH$_3$), 2.92 [d, 1 H, allyl$_{syn}$, ^3J(H–P) = 10.6], 2.99 (br s, 1 H, allyl$_{syn}$), 3.40 (m, 1 H, allyl$_{anti}$), 3.92–4.38 (1 H, allyl$_{anti}$; 2 H, CH$_2$; 4 H, C$_5$H$_4$, superimposed) and 7.05–8.01 (m, 20 H, C$_6$H$_5$); ^{31}P-{^{1}H} (81.02 MHz, CH$_2$Cl$_2$–C$_6$D$_6$), δ 86.3 [s, br, P(Mn)] and 10.3 [d, P(Pd), ^2J(P–P) = 6 Hz].

[(OC)$_2$(η-C$_5$H$_4$Me)Mn(μ-dppm)Pd(CNC$_6$H$_3$Me$_2$-2,6)Cl$_2$] **12a**. To a solution of complex **3** (0.154 g, 0.20 mmol) in CH$_2$Cl$_2$ (10 cm^3) solid 2,6-xylyl isocyanide (0.027 g, 0.20 mmol) was added in three portions. An immediate colour change to yellow was observed and IR monitoring showed quantitative formation of **12a** after 10 min. The volume was concentrated to *ca.* 5 cm^3 and the solution was layered with hexane. Air-stable orange crystals were isolated after 1 d as CH$_2$Cl$_2$ solvates (0.166 g, 86%) (Found: C, 53.85; H, 4.05; N, 1.25. Calc. for C$_{42}$H$_{38}$Cl$_2$MnNO$_2$P$_2$Pd·CH$_2$Cl$_2$: C, 53.35; H, 4.15; N, 1.45%). IR (CH$_2$Cl$_2$): ν(CN) 2205m; ν(CO) 1926s and 1858s; (KBr) ν(CN) 2202m; 1932s and 1864s cm^{-1}. FIR (polyethylene): ν(Pd–Cl) 335w and 296m cm^{-1}. NMR(CDCl$_3$): ^{1}H(300 MHz), δ 1.77 (s, 3 H, C$_5$H$_4$CH$_3$), 2.04 (s, 6 H, CH$_3$), 4.08–4.49 (m, 6 H, C$_5$H$_4$ and dppm) and 6.98–8.01 (m, 23 H, aromatics); ^{31}P-{^{1}H} (121.49 MHz), δ 84.8 [s, P(Mn)] and 23.4 [d, P(Pd), ^2J(P–P) = 4 Hz].

[(OC)$_2$(η-C$_5$H$_4$Me)Mn(μ-dppm)Pd(CNBu^t)Cl$_2$] **12b**. To a solution of complex **3** (0.154 g, 0.20 mmol) in CH$_2$Cl$_2$ (10 cm^3), was slowly added *tert*-butyl isocyanide (0.017 g, 0.20 mmol in 5 cm^3 CH$_2$Cl$_2$). After 10 min the volume was concentrated to *ca.* 5 cm^3. The solution was layered with hexane and kept in a refrigerator for 2 d. Air-stable orange crystals were isolated as CH$_2$Cl$_2$ solvates (0.122 g, 66%) (Found: C, 51.15; H, 4.35; N, 1.55. Calc. for C$_{38}$H$_{38}$Cl$_2$MnNO$_2$P$_2$Pd·CH$_2$Cl$_2$: C, 50.90; H, 4.40; N, 1.50%). IR (CH$_2$Cl$_2$): ν(CN) 2228m; ν(CO) 1926s and 1859s cm^{-1}. FIR (polyethylene): ν(Pd–Cl) 332m and 292s cm^{-1}. NMR (CDCl$_3$): ^{1}H(300 MHz), δ 1.25 (s, 9 H, Bu^t), 1.74 (s, 3 H, C$_5$H$_4$CH$_3$), 4.18–4.39 (m, 6 H, C$_5$H$_4$ and dppm) and 6.99–7.49 (m, 20 H, aromatics); ^{31}P-{^{1}H} (121.49 MHz), δ 85.2 [br s, P(Mn)] and 22.8 [s, P(Pd), ^2J(P–P) not resolved].

[(OC)$_2$(η-C$_5$H$_4$Me)Mn(μ-dppm)Pd(NHC$_3$H$_6$)Cl$_2$] **13**. A rapid reaction occurred when azetidine (0.008 g, 0.15 mmol) was added to a solution of complex **3** (0.093 g, 0.10 mmol) in CH$_2$Cl$_2$ (6 cm^3). Air-stable orange crystals of the product solvated with 2CH$_2$Cl$_2$ were isolated after layering the solution with hexane. Yield 0.084 g (86%). They progressively lose CH$_2$Cl$_2$ on standing (Found: C, 51.40; H, 4.40; N, 1.75. Calc. for C$_{36}$H$_{36}$Cl$_2$MnNO$_2$P$_2$Pd·0.5CH$_2$Cl$_2$: C, 51.50; H, 4.40; N, 1.65%). IR (KBr): ν(NH) 3208w; ν(CO) 1920s and 1852s cm^{-1}. FIR (polyethylene): ν(Pd–Cl) 348s cm^{-1}. NMR (CDCl$_3$): ^{1}H-(300 MHz), δ 1.71 (s, 3 H, C$_5$H$_4$CH$_3$), 2.35 (m, 2 H, CH$_2$), 3.55 (m, 2 H, CH$_2$), 3.95 (m, 2 H, CH$_2$), 3.78 [dd, 2 H, CH$_2$, ^2J(P–H) = 7.1 and 13.1], 4.05–4.15 (m, 4 H, C$_5$H$_4$) and 7.10–7.65 (m, 21 H, aromatics and obscured NH); ^{31}P-{^{1}H} (121.49 MHz), δ 88.2 [d, P(Mn), ^2J(P–P) = 26 Hz] and 13.1 [d, P(Pd)].

[(OC)$_2$(η-C$_5$H$_4$Me)Mn(μ-dppm)AuBr] **14**. The preparation and work-up were similar to those for complex **7**, using **1** (0.100 g, 0.174 mmol) and [AuBr(tht)] (0.064 g, 0.174 mmol), yield 0.13 g (87%) (Found: C, 43.40; H, 3.40. Calc. for C$_{33}$H$_{29}$AuBrMnO$_2$P$_2$·CH$_2$Cl$_2$: C, 43.60; H, 3.35%). IR (KBr): ν(CO) 1925 (sh), 1917s, 1856 (sh) and 1847s cm^{-1}. FIR (polyethylene): 364m and 359s; ν(AuBr) 232m cm^{-1}. NMR: ^{1}H(200 MHz, CD$_2$Cl$_2$), δ 1.73 (s, 3 H, CH$_3$), 3.54 [dd, 2 H, CH$_2$, ^2J(H–P) = 11.1, 5.7], 4.02 (m, 2 H, C$_5$H$_4$), 4.10 (m, 2 H, C$_5$H$_4$) and 7.32–7.71 (m, 20 H, C$_6$H$_5$); ^{31}P-{^{1}H} (81.02 MHz, CH$_2$Cl$_2$–CD$_2$Cl$_2$, 305 K), δ 87.9 [br, P(Mn)] and 23.0 [br, P(Au)]; (253 K), δ 85.1 [br, d, ^2J(P–P) = 7] and 20.6 [d, ^2J(P–P) = 7 Hz].

[(OC)$_2$(η-C$_5$H$_4$Me)Mn(μ-dppm)AuFe{Si(OMe)$_3$}(CO)$_3$-(PPh$_3$)] **15**. A solution of K[Fe{Si(OMe)$_3$}(CO)$_3$(PPh$_3$)] (0.098 g, 0.174 mmol) in thf (10 cm^3) was added to a solution of complex **14** (0.148 g, 0.174 mmol) at 0 °C. After warming to room temperature the solution was stirred for 1 h and filtered to remove KCl. The solvent was evaporated under reduced pressure and the residue extracted with toluene (5 cm^3). The same volume of hexane was added and the solution was left at −30 °C for 24 h to yield yellow crystals (0.20 g, 90%) (Found: C, 53.70; H, 4.35. Calc. for C$_{57}$H$_{53}$AuFeMnO$_8$P$_3$Si: C, 52.90; H, 4.15%). IR (KBr): ν(CO) 1971m, 1911s and 1887s [Fe(CO)$_3$]; 1937vs and 1862vs [Mn(CO)$_2$]; (toluene) ν(CO) 1974m, 1913s and 1887s [Fe(CO)$_3$]; 1922vs and 1859vs cm^{-1} [Mn(CO)$_2$]. FIR (polyethylene): 351m cm^{-1}. NMR: ^{1}H(200 MHz, CD$_2$Cl$_2$), δ 1.77 (s, 3 H, CH$_3$), 3.56 [dd, 2 H, CH$_2$, ^2J(H–P) = 10.3, 5.6], 3.64 (s, 9 H, OMe), 3.97 (m, 2 H, C$_5$H$_4$), 4.08 (m, 2 H, C$_5$H$_4$) and 7.09–7.60 (m, 35 H, C$_6$H$_5$); ^{31}P-{^{1}H} (81.02 MHz, CH$_2$Cl$_2$–CD$_2$Cl$_2$), δ 82.1 [d, br, P^3(Mn), ^2J(P^2–P^3) = 16], 63.3 [d, P^1(Fe), ^3J(P^1–P^2) = 11] and 22.2 [dd, P^2(Au), ^2J(P^2– P^3) = 16, ^3J(P^2–P^1) = 11 Hz].

[Pt$_2$W$_2$(η-C$_5$H$_4$Me)$_2$(μ$_3$-CO)$_2$(μ-CO)$_4${(μ-dppm)Mn-(η-C$_5$H$_4$Me)(CO)$_2$}$_2$] **16**. Solid complex **1** (0.100 g, 0.174 mmol) and *trans*-[Pt{W(η-C$_5$H$_4$Me)(CO)$_3$}$_2$(NCPh)$_2$] (0.195 g, 0.174 mmol) were mixed and toluene (5 cm^3) was added. The mixture was stirred for 24 h under exclusion of light. The resulting dark brown solution was filtered and evaporated to 1 cm^3. Slow diffusion of hexane into a CH$_2$Cl$_2$ solution yielded brown crystals (0.15 g, 71%) (Found: C, 42.35; H, 2.80. Calc. for C$_{84}$H$_{72}$Mn$_2$O$_{10}$P$_4$Pt$_2$W$_2$·2.5CH$_2$Cl$_2$: C, 42.50; H, 3.15%). IR

Table 4 X-Ray crystallographic data for complexes **12a**·CHCl$_3$ and **13**·2CH$_2$Cl$_2$ [a]

	12a·CHCl$_3$	**13**·2CH$_2$Cl$_2$
Formula	C$_{42}$H$_{38}$Cl$_2$MnNO$_2$P$_2$Pd·CHCl$_3$	C$_{36}$H$_{36}$Cl$_2$MnNO$_2$P$_2$Pd·2CH$_2$Cl$_2$
M	1012.6	978.8
Space group	$P2_1/n$	$P2_1/c$
Crystal dimensions/mm	0.10 × 0.20 × 0.10	0.40 × 0.30 × 0.20
a/Å	9.129(2)	13.829(4)
b/Å	18.039(4)	11.054(3)
c/Å	25.835(3)	28.220(8)
β/°	91.90(1)	98.87(2)
U/Å^3	4252(1)	4262(3)
D_c/g cm^{-3}	1.582	1.525
F(000)	1792	1976
μ/cm^{-1}	10.47	11.87
θ limits/°	2–20	2–24
Data collected	4412	5680
Unique data used [$I > 3\sigma(I)$], N	2723	4006
$R = \Sigma(\|\|F_o\| - \|F_c\|\|)/\Sigma\|F_o\|$	0.046	0.072
$R' = [\Sigma w(\|F_o\| - \|F_c\|)^2/\Sigma w\|F_o\|^2]^{\frac{1}{2}}$	0.051	0.100
p	0.04	0.08
Goodness of fit [b]	1.24	1.40
Highest peak in Fourier-difference synthesis/e Å^{-3}	0.62	0.20

[a] Details in common: orange; monoclinic; Z = 4; ω–2θ scan; octants $\pm h, +k, +l$. [b] $[\Sigma w(\|F_o\| - \|F_c\|)^2/(N_o - N_p)]^{\frac{1}{2}}$, where N_o, N_p = number of observations and parameters.

Table 5 Positional parameters and their e.s.d.s for [(OC)$_2$(η-C$_5$H$_4$Me)Mn(μ-dppm)Pd(CNC$_6$H$_3$Me$_2$-2,6)Cl$_2$]·CHCl$_3$ **12a**·CHCl$_3$

Atom	x	y	z	Atom	x	y	z
Pd	−0.078 10(8)	0.068 81(4)	0.185 42(3)	C(23)	0.424(1)	0.121 3(8)	0.403 4(5)
Cl(1)	−0.228 6(3)	0.080 5(2)	0.254 7(1)	O(1)	0.458(1)	0.181 4(6)	0.416 7(4)
Cl(2)	−0.220 0(4)	0.153 0(2)	0.136 8(1)	C(24)	0.262(1)	0.022 2(8)	0.439 2(5)
C(1)	0.034(1)	0.053 1(6)	0.124 4(5)	O(2)	0.192(1)	0.016 9(6)	0.475 5(4)
N	0.093(1)	0.045 5(5)	0.086 0(4)	P(2)	0.197 5(3)	0.074 8(2)	0.334 1(1)
C(2)	0.157(1)	0.040 0(8)	0.038 3(4)	C(25)	0.065(1)	0.128 5(6)	0.369 0(4)
C(3)	0.227(1)	−0.024 9(8)	0.025 2(5)	C(26)	−0.045(1)	0.094 2(6)	0.396 7(4)
C(4)	0.289(2)	−0.027(1)	−0.023 8(7)	C(27)	−0.138(1)	0.134 6(8)	0.426 9(5)
C(5)	0.271(2)	0.031(1)	−0.056 9(7)	C(28)	−0.124(1)	0.209 6(9)	0.430 6(5)
C(6)	0.199(2)	0.096(1)	−0.044 3(6)	C(29)	−0.014(1)	0.245 7(7)	0.404 2(5)
C(7)	0.142(1)	0.101 6(8)	0.004 7(5)	C(30)	0.077(1)	0.204 9(7)	0.374 3(4)
C(8)	0.238(2)	−0.090 5(9)	0.060 9(5)	C(31)	0.240(1)	0.138 7(5)	0.281 3(4)
C(9)	0.063(2)	0.170 9(9)	0.021 6(6)	C(32)	0.128(1)	0.173 2(6)	0.252 1(4)
P(1)	0.051 4(3)	−0.014 5(1)	0.233 3(1)	C(33)	0.164(1)	0.216 0(6)	0.210 2(4)
C(10)	0.232(1)	−0.037 1(6)	0.210 2(4)	C(34)	0.308(2)	0.225 4(6)	0.197 1(5)
C(11)	0.319(1)	0.016 3(6)	0.189 1(4)	C(35)	0.418(1)	0.192 7(6)	0.225 3(5)
C(12)	0.462(1)	0.001 6(6)	0.176 3(4)	C(36)	0.384(1)	0.149 4(6)	0.266 8(4)
C(13)	0.518(1)	−0.069 4(7)	0.183 8(4)	C(37)	0.580(1)	−0.022 3(7)	0.409 0(5)
C(14)	0.431(1)	−0.123 1(6)	0.204 2(5)	C(38)	0.471(1)	−0.074 7(7)	0.406 4(5)
C(15)	0.288(1)	−0.107 8(6)	0.219 0(4)	C(39)	0.409(1)	−0.077 1(7)	0.354 0(5)
C(16)	−0.054(1)	−0.099 3(5)	0.229 2(4)	C(40)	0.486(1)	−0.025 9(7)	0.325 5(5)
C(17)	−0.051(1)	−0.140 9(6)	0.183 9(4)	C(41)	0.590(1)	0.007 6(7)	0.358 8(5)
C(18)	−0.133(1)	−0.201 6(7)	0.177 9(5)	C(42)	0.431(2)	−0.124 8(9)	0.451 0(6)
C(19)	−0.224(1)	−0.225 0(7)	0.215 5(8)	C(43)	0.032(5)	0.253(2)	0.553(1)
C(20)	−0.229(1)	−0.185 6(8)	0.260 1(6)	Cl(3)	0.009 7(9)	0.139 5(5)	0.587 1(3)
C(21)	−0.145(1)	−0.121 8(6)	0.267 6(4)	Cl(4)	−0.044(2)	0.290 2(8)	0.555 4(5)
C(22)	0.077(1)	0.002 9(6)	0.303 4(4)	Cl(5)	0.185(3)	0.212(1)	0.524 7(9)
Mn	0.377 5(2)	0.031 37(9)	0.385 90(6)				

Table 6 Positional parameters and their e.s.d.s for [(OC)$_2$(η-C$_5$H$_4$Me)Mn(μ-dppm)Pd(NHC$_3$H$_6$)Cl$_2$]·2CH$_2$Cl$_2$ **13**·2CH$_2$Cl$_2$

Atom	x	y	z	Atom	x	y	z
Pd	0.405 46(6)	0.444 36(8)	0.414 59(3)	C(19)	0.127(1)	0.608(1)	0.418 0(6)
Mn	0.061 3(1)	0.077 7(2)	0.398 06(6)	C(20)	0.107(1)	0.514(1)	0.445 8(5)
Cl(1)	0.483 9(3)	0.541 9(3)	0.359 9(1)	C(21)	0.116 2(9)	0.394(1)	0.430 1(4)
Cl(2)	0.357 2(2)	0.340 0(3)	0.477 8(1)	C(22)	0.491 5(8)	0.176(1)	0.387 6(4)
P(1)	0.151 6(2)	0.214 3(3)	0.367 44(9)	C(23)	0.488 9(9)	0.069(1)	0.413 0(6)
P(2)	0.385 0(2)	0.273 8(3)	0.370 26(9)	C(24)	0.577(1)	0.003(1)	0.425 8(7)
C(1)	0.132 6(9)	−0.039(1)	0.380 0(5)	C(25)	0.661 7(9)	0.042(1)	0.411 4(6)
O(1)	0.178 6(8)	−0.115 8(8)	0.368 0(4)	C(26)	0.663 5(9)	0.149(2)	0.387 7(6)
C(2)	0.137 1(8)	0.082(1)	0.453 8(4)	C(27)	0.579 5(9)	0.216(1)	0.375 3(5)
O(2)	0.187 0(7)	0.080(1)	0.491 0(3)	C(28)	0.376 5(8)	0.283(1)	0.305 4(4)
C(3)	−0.071 0(8)	0.138(1)	0.423 7(4)	C(29)	0.405(1)	0.183(1)	0.281 1(5)
C(4)	−0.070 3(9)	0.009(1)	0.419 2(5)	C(30)	0.394(1)	0.193(2)	0.229 1(5)
C(5)	−0.070 3(8)	−0.021(1)	0.372 0(5)	C(31)	0.357(1)	0.294(2)	0.206 5(6)
C(6)	−0.067 8(8)	0.085(1)	0.345 6(5)	C(32)	0.332(2)	0.390(2)	0.231 1(5)
C(7)	−0.068 3(8)	0.184(1)	0.376 9(5)	C(33)	0.340(1)	0.385(2)	0.280 4(4)
C(8)	−0.081(1)	0.207(2)	0.468 8(6)	N	0.427 1(7)	0.603 1(9)	0.456 2(3)
C(9)	0.283 6(7)	0.177(1)	0.381 0(4)	C(34)	0.367(1)	0.637(1)	0.494 4(5)
C(10)	0.121 9(8)	0.217(1)	0.302 5(4)	C(35)	0.400(1)	0.722(1)	0.433 6(6)
C(11)	0.050 0(9)	0.296(1)	0.279 9(4)	C(36)	0.364(1)	0.766(2)	0.477 8(6)
C(12)	0.018(1)	0.282(2)	0.230 3(5)	C(37)	0.265(1)	0.093(2)	0.086 3(7)
C(13)	0.055(1)	0.195(2)	0.205 1(5)	Cl(3)	0.176 9(7)	0.206 8(9)	0.081 8(4)
C(14)	0.124(1)	0.120(2)	0.226 7(5)	Cl(4)	0.212 4(7)	−0.035 6(9)	0.105 0(3)
C(15)	0.156 4(9)	0.131(1)	0.274 9(4)	C(38)	0.648(1)	0.241(2)	0.733(1)
C(16)	0.142 9(7)	0.372(1)	0.386 6(4)	Cl(5)	0.620(1)	0.135(2)	0.689(1)
C(17)	0.165 2(9)	0.469(1)	0.359 8(5)	Cl(6)	0.764(1)	0.217(2)	0.247(1)
C(18)	0.157(1)	0.587(1)	0.375 9(5)				

(KBr): ν(CO) 1814s, 1790s and 1738s [W(CO)$_3$]; 1926vs and 1855vs cm^{-1} [Mn(CO)$_2$]. FIR (polyethylene): 399m, 392m, 380vs, 344s, 340m and 225w cm^{-1}. NMR: ^{1}H(200 MHz, CD$_2$Cl$_2$), δ 1.70 (s, 6 H, CH$_3$), 1.82 (s, 6 H, CH$_3$), 3.83, 3.94 [m, 4 H, CH$_2$; 8 H, C$_5$H$_4$(W)], 4.46, 4.55 [m, 8 H, C$_5$H$_4$(Mn)] and 7.09–7.47 (m, 40 H, C$_6$H$_5$); ^{31}P-{^{1}H} (81.02 MHz, toluene–C$_6$D$_6$), δ 91.9 [m, AA′MM′, P(Mn), ^2J(P–^{195}Pt) = 125] and 42.8 [m, AA′MM′X (X = Pt), P(Pt), ^3J(P–P) = 117, ^1J(P–^{195}Pt) = 4616, ^2J(P–^{195}Pt) *ca.* 110 Hz].

Crystal Structure Determinations.—Suitable single crystals of complexes **12a**·CHCl$_3$ and **13**·2CH$_2$Cl$_2$ were obtained by slow diffusion of hexane into CHCl$_3$ or CH$_2$Cl$_2$ solutions, respectively, at 5 °C. For each compound, a single crystal was cut from a cluster of crystals and mounted on a rotation-free goniometer head. Systematic searches in reciprocal space using an Enraf-Nonius CAD4-F automatic diffractometer showed that crystals of **12a**·CHCl$_3$ and **13**·2CH$_2$Cl$_2$ belong to the monoclinic system (Table 4). Quantitative data were obtained at room temperature using a monochromatic Mo-Kα radiation source (λ = 0.710 73 Å). The resulting data sets were transferred to a VAX computer, and for all subsequent calculations the Enraf-Nonius SDP/VAX package[53] was used. Three standard reflections measured every hour during the entire data collection periods showed no significant trends. The raw data were converted into intensities and corrected for Lorentz, polarization and absorption factors, the latter computed from ψ scans of four reflections. The structures were solved using the heavy-atom method. After refinement of the heavy atoms, Fourier difference maps revealed maximas of residual electronic density close to the positions expected for hydrogen atoms; they were introduced in structure-factor calculations as fixed contributors (C–H 1.08 Å in **12a**·$CHCl_3$ and 0.95 Å in **13**·$2CH_2Cl_2$) with isotropic thermal parameters such as $B(H) = 5$ Å^2 (**12a**·$CHCl_3$) or 1.3 $B_{equiv}(C)$ Å^2 (**13**·$2CH_2Cl_2$). The solvent hydrogen atoms were omitted. Full least-squares refinements; weighting scheme $w = 1/\sigma^2(F)$, $\sigma^2(F^2) = \sigma^2_{counts} + (pI)^2$. A final difference map revealed no significant maxima. The scattering-factor coefficients and anomalous dispersion coefficients were taken from ref. 54. Atomic coordinates are given in Tables 5 and 6.

Additional material available from the Cambridge Crystallographic Data Centre comprises H-atom coordinates, thermal parameters and remaining bond lengths and angles.

Acknowledgements

We are indebted to Dr. G. Giorgi (Centro Interdipartimentale di Analisi e Determinazioni Strutturali, Università di Siena) for mass spectrometric studies. We thank the Centre National de la Recherche Scientifique (Paris) and the Commission of the European Communities (Contract No. ST2J-0479) for financial support and Johnson Matthey plc for a generous loan of $PdCl_2$.

References

1 D. F. Shriver, H. D. Kaesz and R. D. Adams, *The Chemistry of Metal Cluster Complexes*. VCH, Weinheim, 1990; P. Braunstein, in *Perspectives in Coordination Chemistry*, eds. A. F. Williams, C. Floriani and A. E. Merbach, Helvetica Chimica Acta Verlag and VCH, Basel and Weinheim, 1992, pp. 67–107 and refs. therein.
2 R. J. Puddephatt, *Chem. Soc. Rev.*, 1983, 99; B. Chaudret, B. Delavaux and R. Poilblanc, *Coord. Chem. Rev.*, 1988, **86**, 191; P. Braunstein, C. de Méric de Bellefon and B. Oswald, *Inorg. Chem.*, 1993, **32**, 1638 and refs. therein.
3 (*a*) P. Braunstein, M. Knorr, A. Tiripicchio and M. Tiripicchio Camellini, *Angew. Chem., Int. Ed. Engl.*, 1989, **28**, 1361; (*b*) P. Braunstein, M. Knorr, E. Villarroya and J. Fischer, *New J. Chem.*, 1990, **14**, 583; (*c*) P. Braunstein, M. Knorr, H. Piana and U. Schubert, *Organometallics*, 1991, **10**, 828; (*d*) P. Braunstein, M. Knorr, E. Villarroya, A. De Cian and J. Fischer, *Organometallics*, 1991, **10**, 3714; (*e*) P. Braunstein, M. Knorr, U. Schubert, M. Lanfranchi and A. Tiripicchio, *J. Chem. Soc., Dalton Trans.*, 1991, 1507; (*f*) P. Braunstein, L. Douce, M. Knorr, M. Strampfer, M. Lanfranchi and A. Tiripicchio, *J. Chem. Soc., Dalton Trans.*, 1992, 331; (*g*) P. Braunstein, E. Colomer, M. Knorr, A. Tiripicchio and M. Tiripicchio-Camellini, *J. Chem. Soc., Dalton Trans.*, 1992, 903; (*h*) G. Reinhard, B. Hirle, U. Schubert, M. Knorr, P. Braunstein, A. De Cian and J. Fischer, *Inorg. Chem.*, 1993, **32**, 1656; (*i*) F. Balegroune, P. Braunstein, L. Douce, Y. Dusausoy, D. Grandjean, M. Knorr and M. Strampfer, *J. Cluster Sci.*, 1992, **3**, 275.
4 A. M. Arif, D. J. Chandler and R. A. Jones, *Inorg. Chem.*, 1987, **26**, 1780.
5 H. Schäfer, W. Leske and G. Mattern, *Z. Anorg. Allg. Chem.*, 1988, **557**, 59; C. Barre, M. M. Kubicki, J.-C. Leblanc and C. Moise, *Inorg. Chem.*, 1990, **29**, 5244; A. Strube, J. Heuser, G. Huttner and H. Lang, *J. Organomet. Chem.*, 1988, **356**, C9.
6 K. A. E. O'Callaghan, S. J. Brown, J. A. Page, M. C. Baird, T. C. Richards and W. E. Geiger, *Organometallics*, 1991, **10**, 3119.
7 (*a*) M. Tilset, *J. Am. Chem. Soc.*, 1992, **114**, 2740; (*b*) M. Tilset, A. A. Zlota, K. Folting and K. G. Caulton, *J. Am. Chem. Soc.*, 1993, **115**, 4113.
8 N. A. Cooley, K. A. Watson, S. Fortier and M. C. Baird, *Organometallics*, 1986, **5**, 2563.
9 S. Fortier, M. C. Baird, K. F. Preston, J. R. Morton, T. Ziegler, T. J. Jaeger, W. C. Watkins, J. H. MacNeil, K. A. Watson, K. Hensel, Y. Le Page, J.-P. Charland and A. J. Williams, *J. Am. Chem. Soc.*, 1991, **113**, 542.
10 (*a*) N. G. Connelly and M. D. Kitchen, *J. Chem. Soc., Dalton Trans.*, 1977, 931; (*b*) J. W. Hershberger, R. J. Klingler and J. K. Kochi, *J. Am. Chem. Soc.*, 1983, **105**, 61; (*c*) W. E. Geiger, C. G. Atwood and T. T. Chin, in *Molecular Electrochemistry of Inorganic, Bioinorganic and Organometallic Compounds*, NATO ASI Ser. C, eds. A. J. L. Pombeiro and J. A. McCleverty, Kluwer Academic Press, Dordrecht, 1993, vol. 385, pp. 519–532; (*d*) C. G. Atwood, W. E. Geiger and A. L. Rheingold, *J. Am. Chem. Soc.*, 1993, **115**, 5310.
11 N. G. Connelly, K. A. Hassard, B. J. Dunne, A. G. Orpen, S. J. Raven, G. A. Carriedo and V. Riera, *J. Chem. Soc., Dalton Trans.*, 1988, 1623; G. A. Carriedo, N. G. Connelly, M. C. Crespo, I. C. Quarmby, V. Riera and G. H. Worth, *J. Chem. Soc., Dalton Trans.*, 1991, 315; F. L. Atkinson, A. Christofides, N. G. Connelly, H. J. Lawson, A. C. Loyns, A. G. Orpen, G. M. Rosair and G. H. Worth, *J. Chem. Soc., Dalton Trans.*, 1993, 1441.
12 (*a*) W. A. Herrmann, D. Andrejewski and E. Herdtweck, *J. Organomet. Chem.*, 1987, **319**, 183; (*b*) A. J. Hart-Davis and W. A. G. Graham, *J. Am. Chem. Soc.*, 1971, **94**, 4388.
13 F. A. Cotton and G. Wilkinson, *Advanced Inorganic Chemistry*, 5th edn., Wiley-Interscience, New York, 1988, p. 1037.
14 W. A. Schenk and G. H. J. Hilpert, *Chem. Ber.*, 1991, **124**, 433.
15 G. E. Coates and G. Parkin, *J. Chem. Soc.*, 1963, 421.
16 P. Kubacek, R. Hoffmann and Z. Havlas, *Organometallics*, 1982, **1**, 180.
17 E. Kunz, M. Knorr, J. Willnecker and U. Schubert, *New J. Chem.*, 1988, **12**, 467.
18 R. Bender, P. Braunstein, J.-M. Jud and Y. Dusausoy, *Inorg. Chem.*, (*a*) 1983, **22**, 3394; (*b*) 1984, **23**, 4489.
19 P. Hofmann and H. R. Schmidt, *Angew. Chem., Int. Ed. Engl.*, 1986, **25**, 837.
20 A. L. Sargent and M. B. Hall, *J. Am. Chem. Soc.*, 1989, **111**, 1563.
21 D. L. Thorn and R. Hoffmann, *J. Am. Chem. Soc.*, 1978, **100**, 2079.
22 (*a*) G. Huttner, J. Schneider, H.-D. Müller, G. Mohr, J. von Seyerl and L. Wohlfahrt, *Angew. Chem., Int. Ed. Engl.*, 1979, **18**, 76; (*b*) J. Schneider and G. Huttner, *Chem. Ber.*, 1983, **116**, 917; (*c*) R. P. Planalp and H. Vahrenkamp, *Organometallics*, 1987, **6**, 492; (*d*) P. Braunstein, C. de Méric de Bellefon, S.-E. Bouaoud, D. Grandjean, J.-F. Halet and J.-Y. Saillard, *J. Am. Chem. Soc.*, 1991, **113**, 5282; (*e*) L. J. Farrugia, *J. Cluster Sci.*, 1992, **3**, 361.
23 (*a*) A. J. Naaktgeboren, R. J. M. Nolte and W. Drenth, *J. Am. Chem. Soc.*, 1980, **102**, 3350; (*b*) B. L. Shaw, M. J. Smith, G. N. Stretton and M. Thornton-Pett, *J. Chem. Soc., Dalton Trans.*, 1988, 2099.
24 D. M. Adams and P. J. Chandler, *Chem. Ind. (London)*, 1965, 269.
25 F. H. Jardine and P. S. Sheridan, in *Comprehensive Coordination Chemistry*, eds. G. Wilkinson, R. D. Gillard and J. A. McCleverty, Pergamon, Oxford, 1987, vol. 4, p. 901.
26 R. A. Hoffmann, S. Forsen and B. Gestblom, in *NMR Basic Principles and Progress*, eds. P. Diehl, E. Fluck and R. Kosfeld, Springer, Berlin, 1971, vol. 5, pp. 1–165.
27 M. D. Curtis, W. M. Butler and J. Greene, *Inorg. Chem.*, 1978, **17**, 2928; R. C. Schnabel and D. M. Roddick, *Inorg. Chem.*, 1993, **32**, 1513.
28 P. S. Pregosin, in *Phosphorus-31 NMR Spectroscopy in Stereochemical Analysis*, VCH, Weinheim, 1987, p. 465.
29 (*a*) E. H. Wong, F. C. Bradley, L. Prasad and E. J. Gabe, *J. Organomet. Chem.*, 1984, **263**, 167; (*b*) L. Manojlovic-Muir, A. N. Henderson, I. Treurnicht and R. J. Puddephatt, *Organometallics*, 1989, **8**, 2055.
30 (*a*) F. Calderazzo, I. P. Mavani, D. Vitali, I. Bernal, J. D. Korp and J. L. Atwood, *J. Organomet. Chem.*, 1978, **160**, 207; (*b*) E. W. Abel and G. Wilkinson, *J. Chem. Soc.*, 1959, 1501; (*c*) D. A. Edwards and J. Marshalsea, *J. Organomet. Chem.*, 1977, **131**, 73; (*d*) N. M. Boag and H. D. Kaesz, in *Comprehensive Organometallic Chemistry*, eds. G. Wilkinson, F. G. A. Stone and E. W. Abel, Pergamon, Oxford, 1982, vol. 4, p. 161; (*e*) W. Yuquiang, G. Yici and S. Qizhen, *Polyhedron*, 1992, **11**, 2483; (*f*) J. D. Korp, I. Bernal, J. L. Atwood, F. Calderazzo and D. Vitali, *J. Chem. Soc., Dalton Trans.*, 1979, 1492.
31 M. S. Lupin and B. L. Shaw, *J. Chem. Soc. A*, 1968, 741.
32 C. J. F. Barnard, J. A. Daniels, J. Jeffery and R. J. Mawby, *J. Chem. Soc., Dalton Trans.*, 1976, 1861.
33 M. I. Bruce and F. G. A. Stone, *J. Chem. Soc. A*, 1967, 1238; P. Braunstein, D. Matt and Y. Dusausoy, *Inorg. Chem.*, 1983, **22**, 2043; M. Schröder and T. A. Stephenson, in *Comprehensive Coordination Chemistry*, eds. G. Wilkinson, R. D. Gillard and J. A. McCleverty, Pergamon, Oxford, 1987, vol. 4, p. 277; E. Lindner, A. Möckel, H. A. Mayer and R. Fawzi, *Chem. Ber.*, 1992, **125**, 1363.
34 (*a*) J. Powell and B. L. Shaw, *J. Chem. Soc. A*, 1967, 1839; (*b*) P. W. N. M. van Leeuwen, A. P. Praat and M. van Diepen,

J. Organomet. Chem., 1971, **29**, 433; (*c*) M. Sakakibara, Y. Takahashi, S. Sakai and Y. Ishii, *J. Organomet. Chem.*, 1971, **27**, 139; (*d*) A. Albinati, R. W. Kunz, C. J. Ammann and P. S. Pregosin, *Organometallics*, 1991, **10**, 1800.

35 P. Braunstein, T. Faure, M. Knorr, F. Balegroune and D. Grandjean, *J. Organomet. Chem.*, 1993, **462**, 271.

36 R. Bertani, M. Mozzon, F. Benetello, G. Bombieri and R. A. Michelin, *J. Chem. Soc., Dalton Trans.*, 1990, 1197.

37 P. Braunstein and R. J. H. Clark, *J. Chem. Soc., Dalton Trans.*, 1973, 1845; A. G. Jones and D. B. Powell, *Spectrochim. Acta, Part A*, 1974, **30**, 563, 1001.

38 N. Hadj-Bagheri and R. J. Puddephatt, *Inorg. Chem.*, 1989, **28**, 2384.

39 A. T. Hutton, P. G. Pringle and B. L. Shaw, *J. Chem. Soc., Dalton Trans.*, 1985, 1677; A. L. Balch, E. Y. Fung and M. M. Olmstead, *Inorg. Chem.*, 1990, **29**, 3203; S. S. M. Ling, I. R. Jobe, L. Manojlovic-Muir, K. W. Muir and R. J. Puddephatt, *Organometallics*, 1985, **4**, 1198.

40 C. Barbeau, K. Sorrento Dichmann and L. Ricard, *Can. J. Chem.*, 1973, **51**, 3027; M. J. Zaworotko, R. Shakir, J. L. Atwood, V. Sriyunyongwat, S. D. Reynolds and T. A. Albright, *Acta Crystallogr., Sect. B*, 1982, **38**, 1572; O. Orama, *J. Organomet. Chem.*, 1986, **314**, 273; C. Lo Sterzo and J. K. Stille, *Organometallics*, 1990, **9**, 687.

41 A. G. Orpen, L. Brammer, F. H. Allen, O. Kennard, D. G. Watson and R. Taylor, *J. Chem. Soc., Dalton Trans.*, 1989, 51.

42 T. Gennet, D. F. Milner and M. J. Weaver, *J. Phys. Chem.*, 1985, **89**, 2787.

43 J. B. Flanagan, S. Margel, A. J. Bard and F. C. Anson, *J. Am. Chem. Soc.*, 1978, **100**, 4248.

44 R. Jund, P. Lemoine, M. Gross, R. Bender and P. Braunstein, *J. Chem. Soc., Dalton Trans.*, 1985, 711.

45 P. Zanello, G. Opromolla, M. Casarin, M. Herberhold and P. Leitner, *J. Organomet. Chem.*, 1993, **443**, 199.

46 P. Zanello, G. Opromolla, G. Giorgi, J. C. Van De Grampel and H. F. M. Schoo, *Polyhedron*, 1993, **12**, 1329.

47 M. Green, J. A. K. Howard, J. L. Spencer and F. G. A. Stone, *J. Chem. Soc., Chem. Commun.*, 1975, 3; *J. Chem. Soc., Dalton Trans.*, 1977, 271.

48 M. Sakakibara, Y. Takahashi, S. Sakai and Y. Ishii, *Chem. Commun.*, 1969, 396.

49 D. Vitali and F. Calderazzo, *Gazz. Chim. Ital.*, 1972, **102**, 587.

50 A. Mantovani and S. Cenini, *Inorg. Synth.*, 1976, **16**, 51.

51 G. Giordano and R. H. Crabtree, *Inorg. Synth.*, 1979, **19**, 218.

52 R. Uson and A. Laguna, *Organomet. Synth.*, 1986, **3**, 322.

53 B. A. Frenz, in *Computing in Crystallography*, eds. H. Schenk, R. Olthof-Hazekamp, H. Van Koningveld and G. C. Bassi, Delft University Press, Delft, 1978, pp. 64–71.

54 D. T. Cromer and J. T. Waber, *International Tables for X-Ray Crystallography*, Kynoch Press, Birmingham, 1974, vol. 4, Tables 2.2b and 2.3.1.

Received 2nd December 1993; *Paper* 3/07130H